Electronic Supplementary Material (ESI) for Chemical Science.
This journal is © The Royal Society of Chemistry 2019

Supporting information for

A Side-Chain Engineering Strategy for Constructing Fluorescent Dyes with Direct and Ultrafast Self-Delivery to Living Cells

Lifang Guo,[a] Chuanya Li,[a] Hai Shang,[b] Ruoyao Zhang,[a] Xuechen Li,[a] Qing Lu,[a] Xiao Cheng,[c] Zhiqiang Liu,*[a] Jing Zhi Sun,*[c] Xiaoqiang Yu*[a,d]

[a] Center of Bio & Micro/Nano Functional Materials, State Key Laboratory of Crystal Materials, Shandong University. Jinan 250100, P. R. China. Email: yuxq@sdu.edu.cn and zqliu@sdu.edu.cn.

[b] Institute of Robotics, Shanghai Jiao Tong University. Shanghai 200240, P.R. China.

[c] MoE Key Laboratory of Macromolecule Synthesis and Functionalization, Department of Polymer Science and Engineering, Zhejiang University. Hangzhou 310027, P. R. China. Email: sunjz@zju.edu.cn.

[d.] Advanced Medical Research Institute, Shandong University, Jinan 250100, P. R. China.

Contents

Materials

Unless otherwise stated, all solvents and reagents were commercially available used without further purification. Thin-layer chromatography (TLC) analysis was performed on silica gel plates and column chromatography was conducted over silica gel (mesh 200-300), both of which were obtained from the Qingdao Ocean Chemicals. MTT (3-(4, 5-Dimethylthiazol-2-yl)-2, 5-diphenyltetrazolium bromide) was from Sigma. MitoTracker® Deep Red FM (MTDR), Mito-Tracker Green (MTG), Mito-Tracker Red (MTR), Rhodamine123 (Rh123) were purchased from Molecular **SPs**. The ^{1}H NMR and ^{13}C NMR spectra were recorded on a Bruker AVANCE III 300 MHz or 400 MHz Digital NMR Spectrometer, and using DMSO-d_6 as solvent and tetramethylsilane (TMS) as internal reference respectively.

Spectroscopic measurements

The UV-visible-near-IR absorption spectra of dilute solutions were recorded on a Hitachi U-2910 spectrophotometer using a quartz cuvette of 1 cm path length. One-photon fluorescence spectra were obtained on a HITACH F-2700 spectrofluorimeter equipped with a 450-W Xe lamp. Two-photon fluorescence spectra were measured on a SpectroPro300i and the pump laser beam came from a mode-locked Ti: sapphire laser system at the pulse duration of 220 fs, a repetition rate of 76 MHz (Coherent Mira900-D).

The fluorescence quantum yields can be calculated by the following equation (1)[1]:

$$\Phi_{s} = \Phi_r \frac{A_r(\lambda_r)}{A_s(\lambda_s)} \frac{n_s^2}{(n_r^2)} \frac{F_s}{F_r} \qquad (1)$$

Two-photon absorption cross sections are calculated by means of equation (2)[2]:

$$\delta_{s} = \delta_r \frac{\Phi_r}{\Phi_s} \frac{n_r}{n_s} \frac{c_r}{c_s} \frac{F_s}{F_r} \qquad (2)$$

The subscripts s and r refer to the sample and the reference materials, respectively. Φ is the quantum yield, F in equation (1) is the one-photon excited fluorescence integrated emission intensity, while in equation (2), it indicates the two-photon excited fluorescence integral intensity. A stands for the absorbance, and n is the refractive index. δ is the two-photon absorption cross-section value, c is the concentration of the solution. In this paper, fluorescein in aqueous NaOH (pH = 13) was selected as the reference. Its Φ and δ (excitation with 800 nm) are 0.93 and 36GM, respectively.[3]

Calculation methods of molecular frontier orbitals

The geometrically optimized structure and the frontier orbitals of the probe molecules were calculated with Gaussian 09 package.[4] Chemical structures were optimized sequentially with the basic set of PM3, B3LYP/3-21g, B3LYP/6-31g, and cam-B3LYP/TZVP. The frontier molecular orbitals were obtained via TD-DFT calculation of the single point of the optimized structure on the basic set of cam-B3LYP/TZVP TD.

Cytotoxicity measurement

The effects of **SPs** on cell viability were carried out using the methylthiazolyldiphenyl-tetrazolium bromide (MTT), purchased from Dojindo. SiHa cells growing in log phase were seeded into 96-well plates (ca. 1×10^4 cells/well) and allowed to adhere for 24 h. **SPs** (100 μL/well) at different concentrations (200 nM and 1 nM) was added into the wells of the treatment group, and 100 μL/well DMSO diluted in DMEM at corresponding concentrations to the negative control group, respectively. The cells were incubated for 2, 10, and 24 h at 37 °C under 5% CO_2, then 10 μL of MTT was added into each well. After incubation for 4 h, the culture medium in each well was removed and DMSO (100 μL) was added to dissolve the purple crystals. After 20 min, the absorbance was measured at 492 nm with a microplate reader. Finally, the cell survival rate can be calculated using the following equation: Cytotoxic experiment was repeated for four times.

$$Survival\ rate = (A_{Sample} - A_{DMSO})/(A_{Sample} - A_{Blank})$$

Cell culture and staining methods

SiHa and HeLa cells were cultured in H-DMEM supplemented with 10% fetal bovine serum (FBS) and 1% penicillin and streptomycin. Mesenchymal stem cells (MSC) were grown in alpha-MEM supplemented with 10% FBS and 1% penicillin and streptomycin. All above cells were cultured in a 5% CO_2 incubator at 37 ^oC. Before cell staining, all cells were placed on glass coverslips and allowed to adhere for 24 h.

For living cells staining experiment, adherent cells were stained with **SPs** or MTG or MTR (detailed staining concentration and time were illustrated in corresponding figure annotations), and then washed with unbounded **SPs** and imaged with fluorescence microscopy.

For co-staining experiments, cells were treated with MDTR (200 nM, 20 min) followed by rinsed with PBS twice and then stained with **SPs** (200 nM, 10 min), and then washed with unbounded **SPs** and imaged with fluorescence microscopy.

Fluorescence imaging methods

Confocal fluorescence imaging was obtained with Olympus FV 1200 laser confocal microscope. In two-photon experiments, excitation wavelength was 900 nm from a Ti:sapphire femtosecond laser source (Coherent Chamelon Ultra), and the incident power on samples was modified by means of an attenuator and examined with Power Monitor (Coherent). A multiphoton emission filter (FF01-750; Semrock) was used to block the IR laser.

Time-dependent dynamic analysis (TDDA)

Adherent cells were treated with different concentrations **SPs** or MTG or MTR, and then immediately observed by confocal microscopy without a washing step.

Fluorescent recovery after photobleaching (FRAP)

Adherent cells were pre-stained with 200 nM **SPs** for 10 min and washed with PBS twice, and then imaged by confocal microscopy. Next, keeping the imaging position unchanged, 200 nM **SPs** pre-dissolved in medium were added into the cells, and they were immediately observed under confocal microscopy without washing.

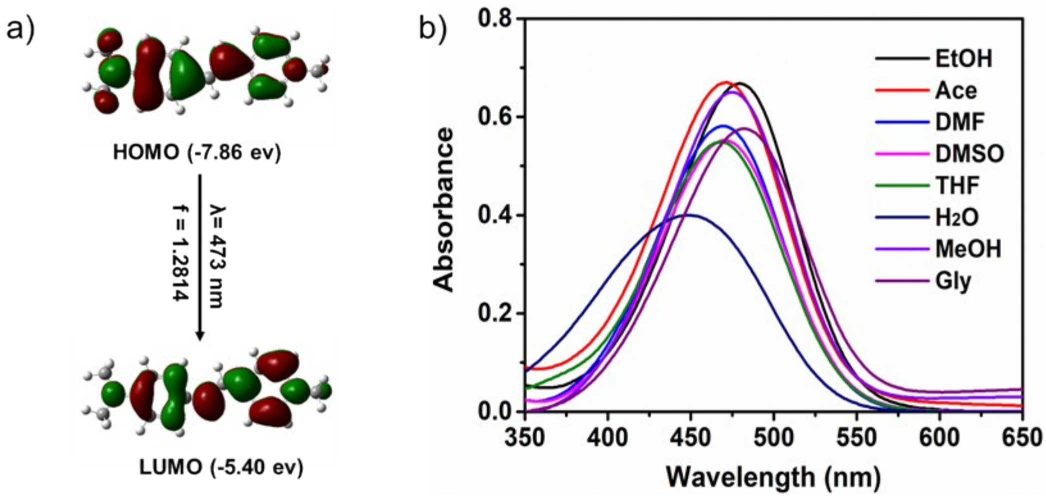

Figure S1. The frontier molecular orbital (a) and absorption spectra (b) of **SP-1**. Testing concentration: 10 μM.

Table S1 Optical properties of **SP-1** compared with references (Rhodamin B and Fluorescein)

Dyes	Solvents	$\lambda^1_{\max}$	$\lambda^2_{\max}$	Φ (%)	δ	$\delta\times\Phi$
SP-1	EtOH	590	607	0.40	315	1.26
	Ace	599	623	0.11	610	0.67
	DMF	599	622	0.20	291	0.58
	DMSO	608	625	0.38	144	0.54
	THF	580	612	1.04	51	0.53
	H_2O	586	616	0.04	1066	0.45
	MeOH	588	617	0.13	271	0.36
	Gly	589	614	7.79	114	8.86
Rhodamin B	MeOH	567	570	59	13	7.67
Fluorescein	NaOH	512	513	89	15	13.35

λ^1_{max}: the maximum OPEF wavelength, λ^2_{max}: the maximum TPEF wavelength (unit: nm); Φ: fluorescence quantum yield; *δ:* the two-photo absorption cross-section; *δ×Φ:* the two-photon active absorption cross-section. The two-photon excitation wavelength: 900 nm.

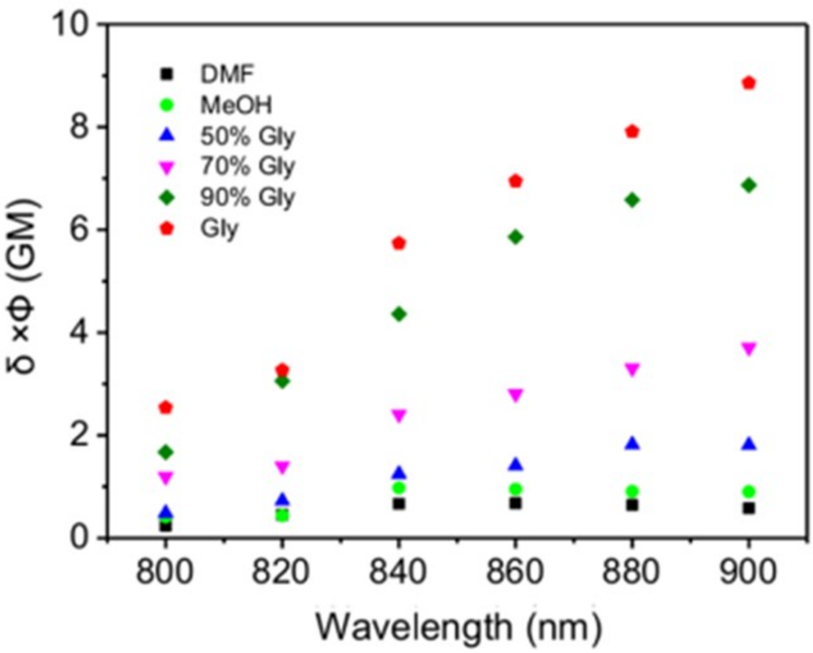

Figure S2. $\delta\times\Phi$ of **SP-1** in various solvents under different two-photon excitation wavelengths from 800 nm to 900 nm.

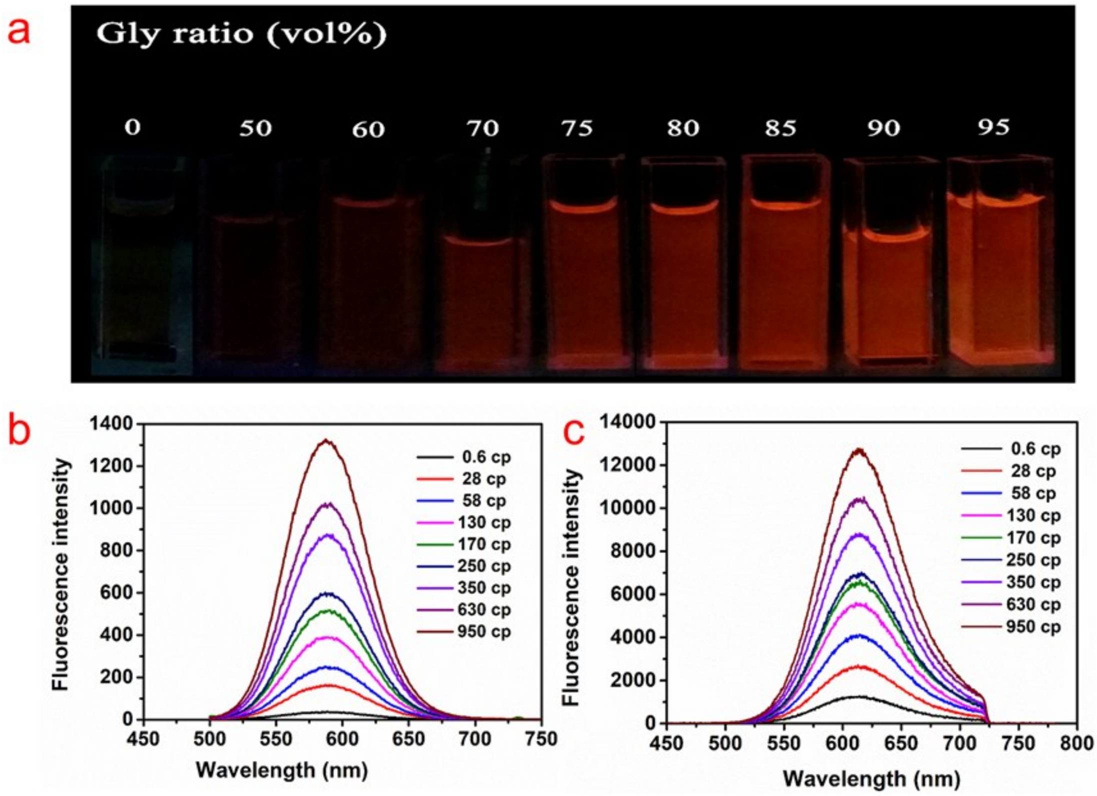

Figure S3. Naked-eye images of **SP-1** under UV light with 365 nm excitation (a), OPEF (b), and TPEF (c) spectra in Gly-MeOH solvents with different viscosity (unit: cp). λ_{ex} (OPEF) = 473 nm; λ_{ex} (TPEF) = 900 nm. Concentration: 10 μM.

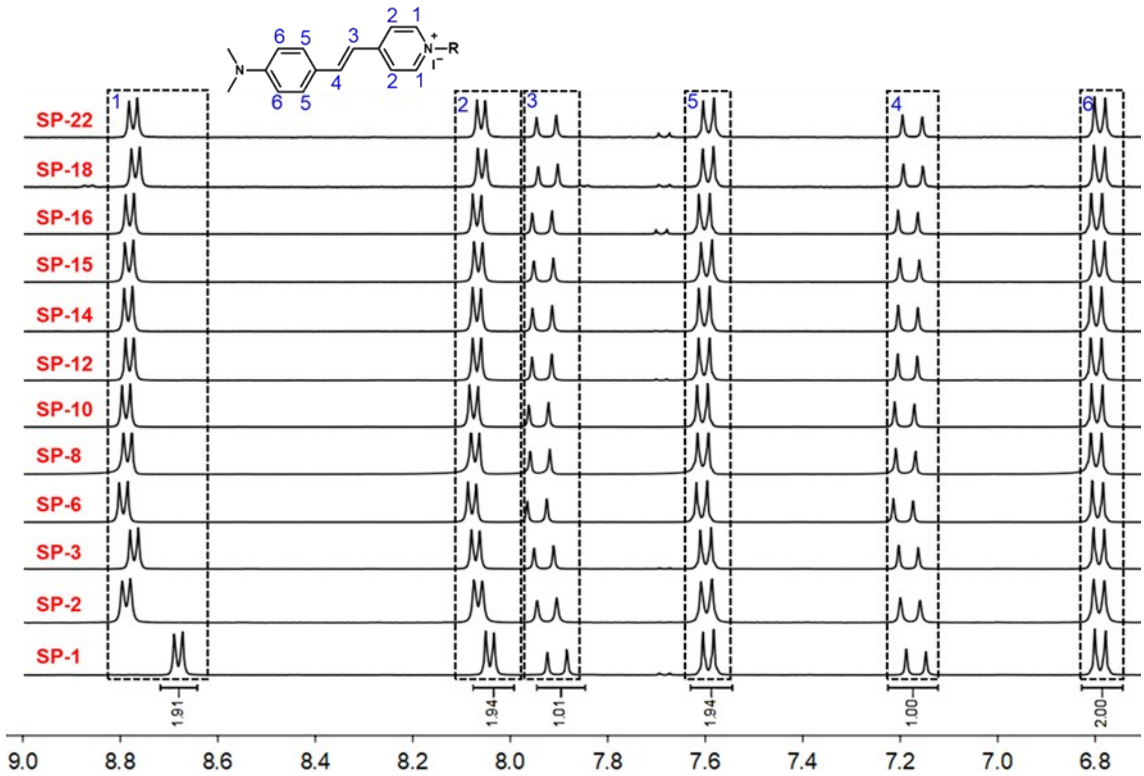

Figure S4. ^{1}H NMR spectra in the low field of chemical shift of total **SPs** with DMSO-d_6 as the solvent.

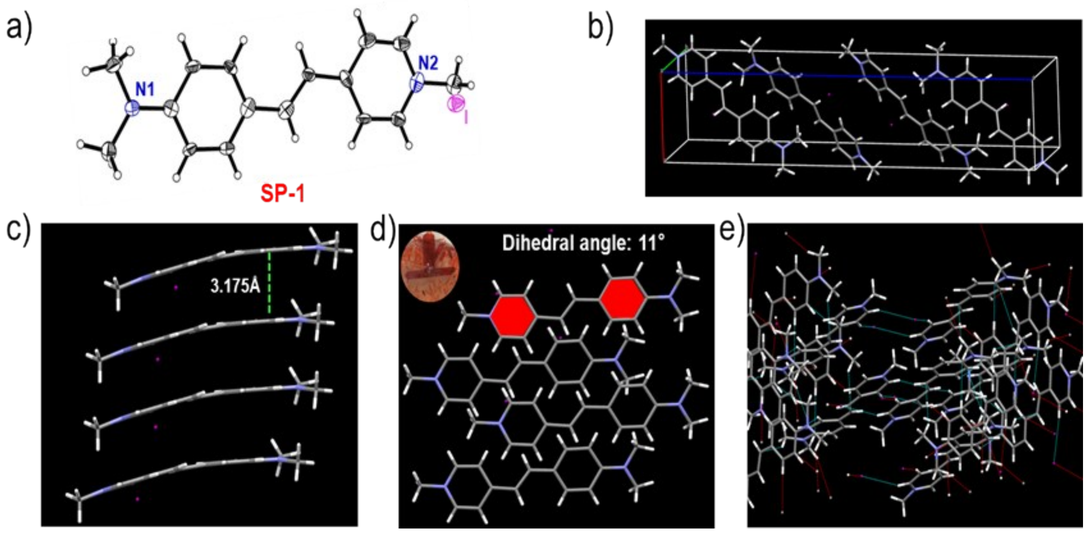

Figure S5. The ORTEP drawing (a), unit cell (b), side view (c), top view (d), and intramolecular short-contact interactions (e) of **SP-1**. The distance between the adjacent parallel benzene rings: 3.175 Å. Dihedral angle between two aromatic rings marked by red: 11˚.

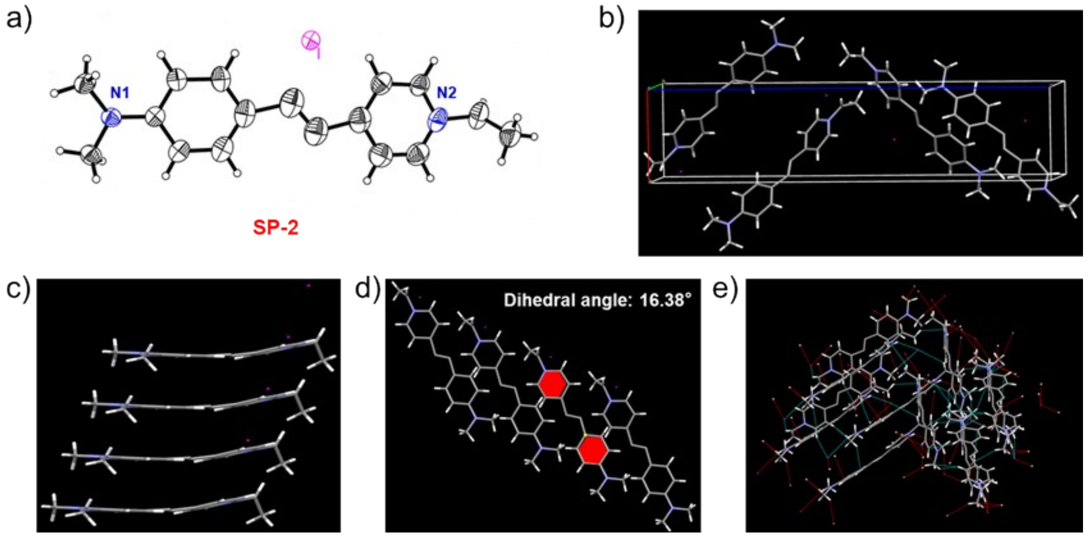

Figure S6. The ORTEP drawing (a), unit cell (b), side view (c), top view (d), and intramolecular short-contact interactions (e) of **SP-2**. The distance between the adjacent parallel benzene rings: 3.374 Å. Dihedral angle between two aromatic rings marked by red: 16.38˚.

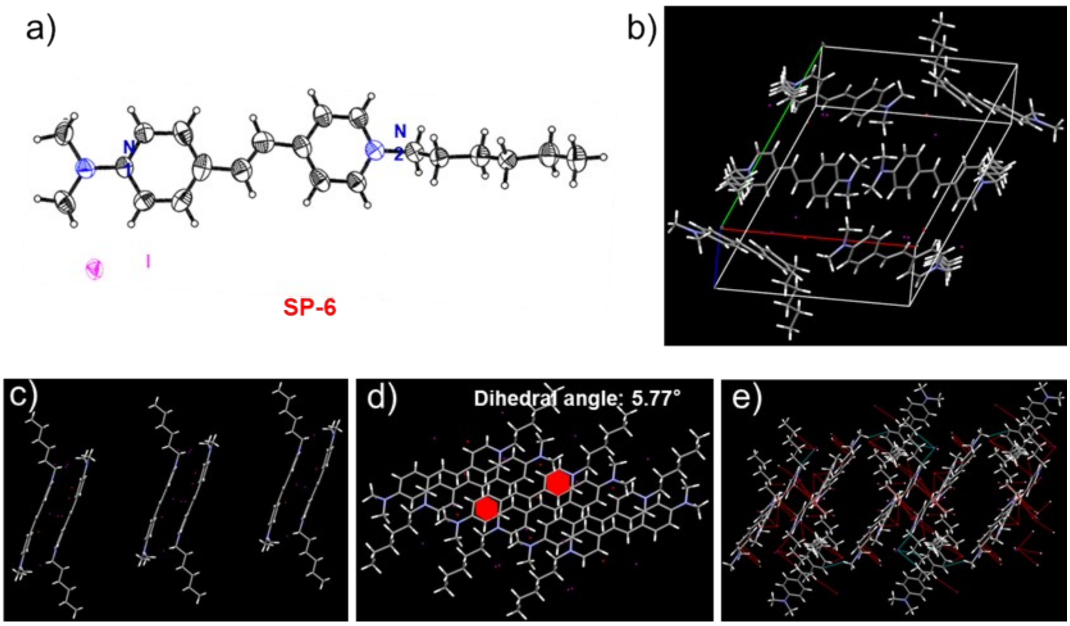

Figure S7. The ORTEP drawing (a), unit cell (b), side view (c), top view (d), and intramolecular short-contact interactions (e) of **SP-6**. The distance of between the adjacent antiparallel benzene rings: 4.092 Å, the distance between the adjacent parallel benzene rings: 13.018 Å. Dihedral angle between two aromatic rings marked by red: 5.77˚.

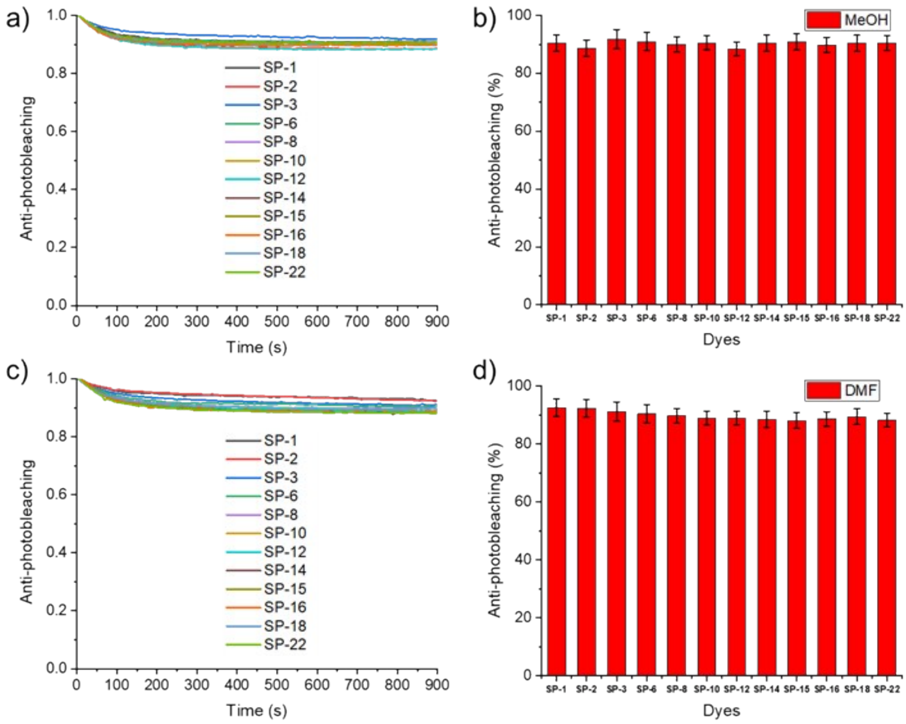

Figure S8. The anti-photobleaching results of **SPs** in two different solvents (a and b: MeOH, c and d: DMF) under continuous excitation with 473 nm laser. a and c: The normalized fluorescence intensity at different time; b and d: the fluorescence intensity ratios of **SPs** at 900 s relative to its original intensity.

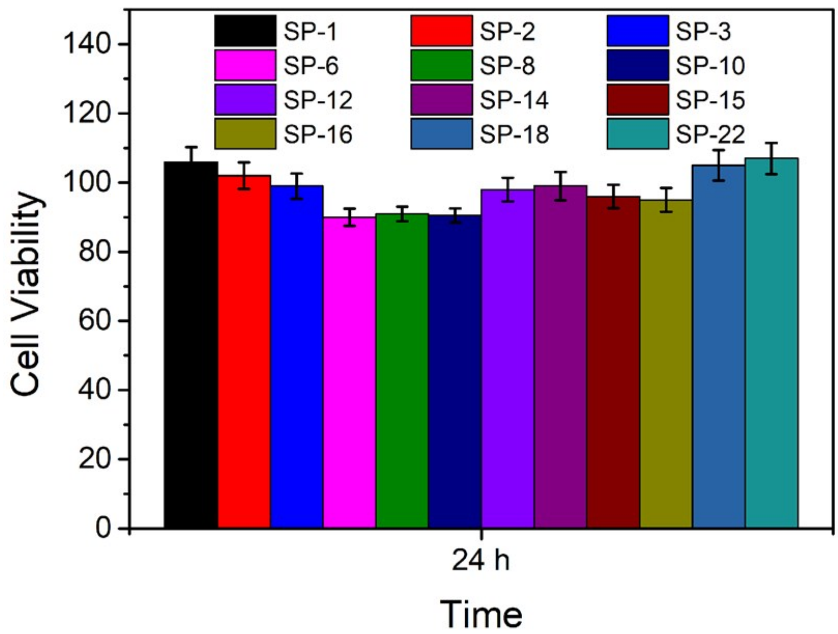

Figure S9. MTT assay of SiHa cells after incubation with 200 nM **SPs** for 24 h.

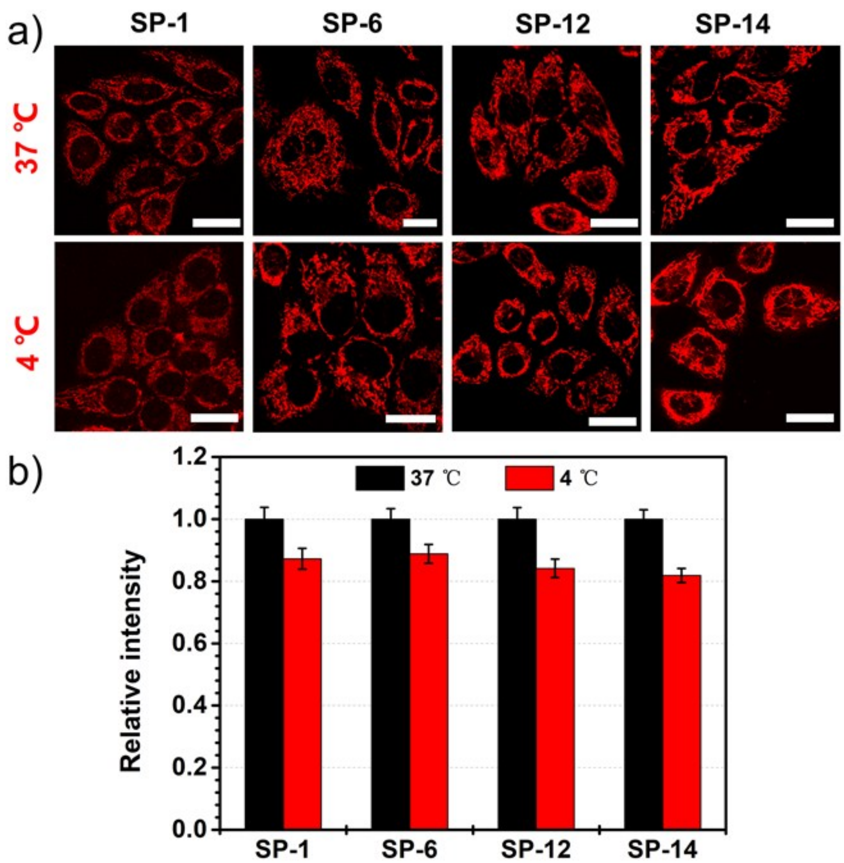

Figure S10. (a) LSCM images of SiHa cells stained with **SP-1**, **SP-6**, **SP-12**, and **SP-14** (200 nM, 10 min) at different incubation temperatures (37℃ and 4℃), and the relative fluorescence intensity (b).

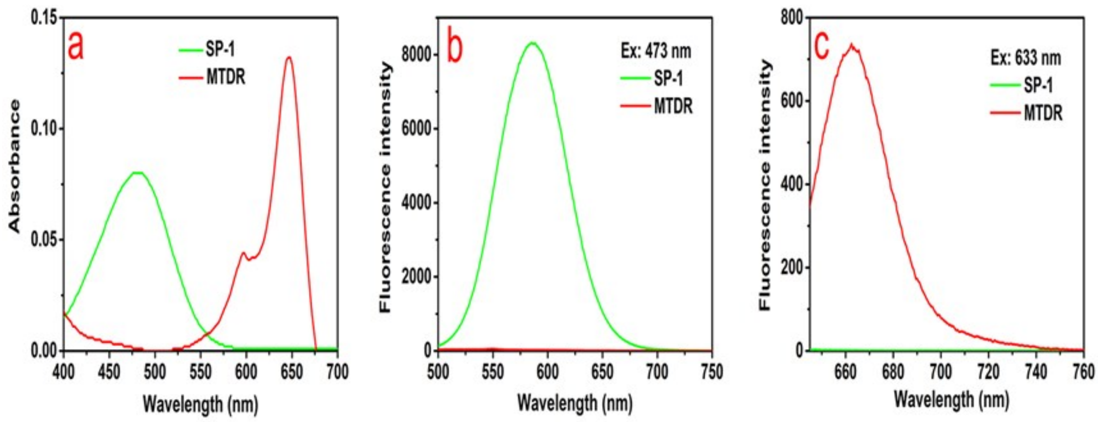

Figure S11. The absorption (a) and emission (b, c) spectra of **SP-1** in mixture solvent of 70% Gly-30% MeOH as well as MTDR in DMSO. Concentration: 10 μM. λ_{ex} (b) = 473 nm; λ_{ex} (c) = 633 nm.

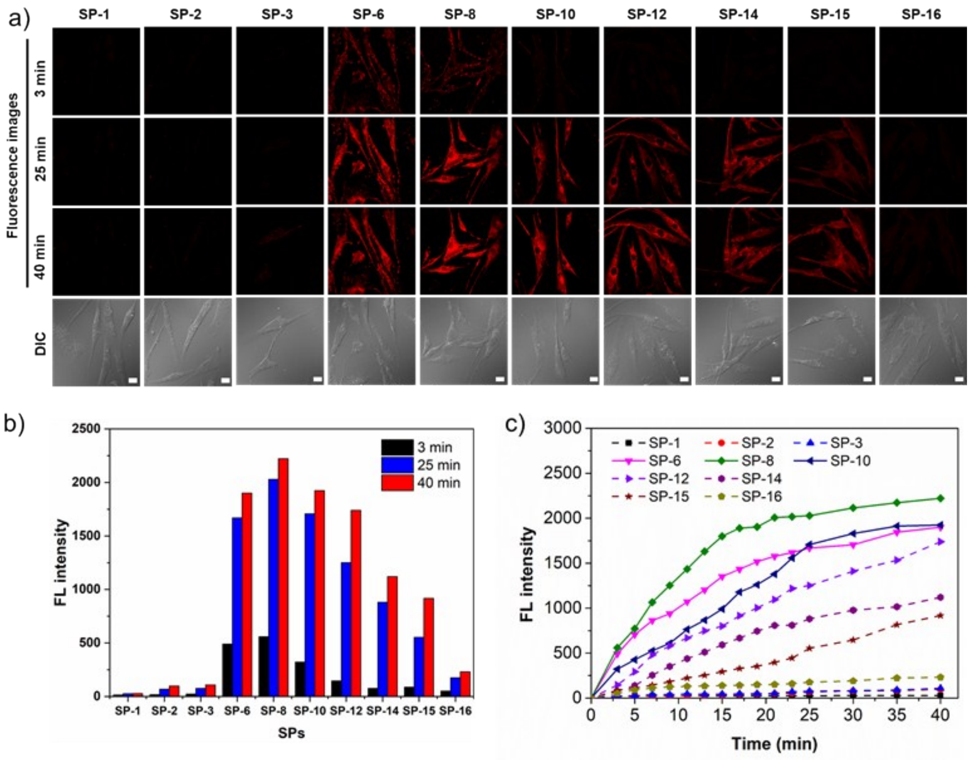

Figure S12. TDDA for diffusion dynamics of **SPs** in MSC. (a) LSCM images of cells stained with **SPs** (200 nM) at different time points (3, 25, and 40 min) and the corresponding DIC images. (b) Time-dependent fluorescence intensity of **SPs** recorded at different time points. (c) The fluorescence intensity plots of **SPs** over time. λ_{ex} = 473 nm, λ_{em} = 550-650 nm. Bar = 20 μm.

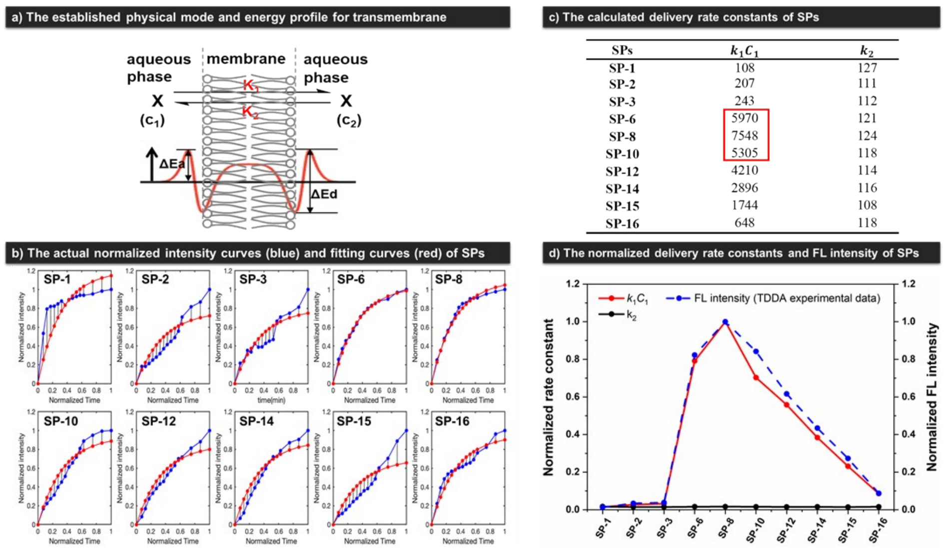

SPs	k_1C_1	k_2
SP-1	108	127
SP-2	207	111
SP-3	243	112
SP-6	5970	121
SP-8	7548	124
SP-10	5305	118
SP-12	4210	114
SP-14	2896	116
SP-15	1744	108
SP-16	648	118

Figure S13. The calculation of delivery rate constants of **SPs** in MSC. (a) Top: the established physical model for the transport of **SPs** through the membrane; Bottom: the corresponding activation energy profile. (b) The experimental intracellular normalized fluorescence intensity curves of **SPs** (blue) at different normalized time as well as the corresponding fitting curves (red). (c) The calculated delivery rate constants of **SPs**. (d) The normalized delivery rate constants and FL intensity at 25 min of TDDA experiment (Figure S12b) of **SPs**.

a)

Dye	Loading conditions	Percentage laser transmission	PMT gain	Offset
SP-6	200 nM / 30 s 100 nM / 3 min 50 nM / 5 min 10 nM / 10 min 5 nM / 15 min 1 nM / 20 min	15%	600	10%

b)

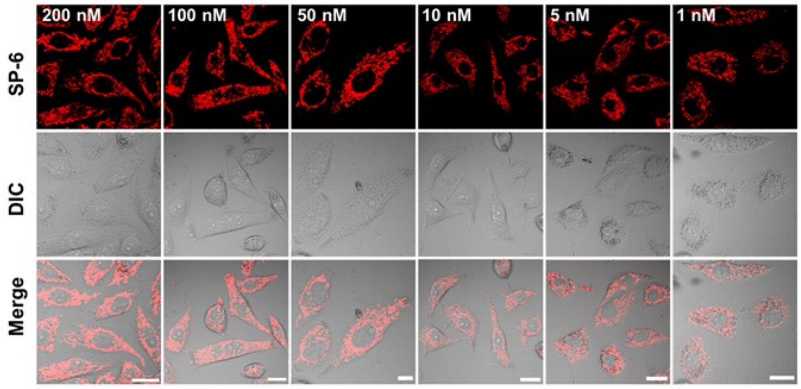

Figure S14. LSCM imaging parameters (a) and images (b) of SiHa cells stained with **SP-6** of different concentrations ranging from 200 nM to 1 nM. λ_{ex} = 473 nm; λ_{em} = 550-650 nm. Bar = 20 μm.

a)

Dye	Loading conditions	Percentage laser transmission	PMT gain	Offset
SP-1	200 nM / 10 min 100 nM / 18 min 50 nM / 30 min 10 nM / 30 min 5 nM / 30 min 1 nM / 30 min	15%	600	10%

b)

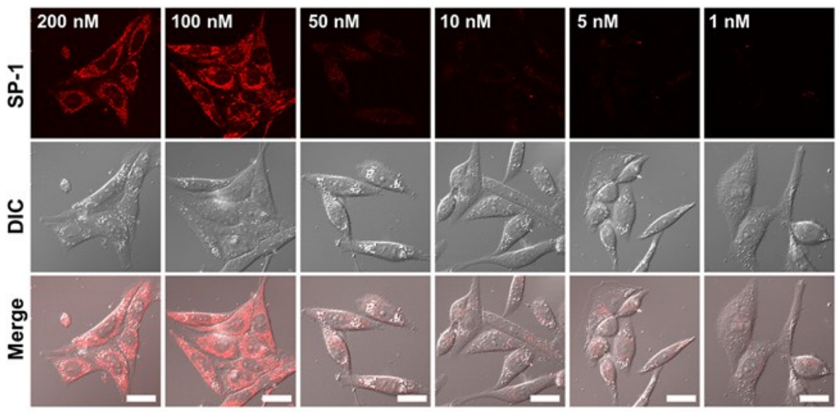

Figure S15. LSCM imaging parameters (a) and images (b) of SiHa cells stained with **SP-8** of different concentrations ranging from 200 nM to 1 nM. λ_{ex} = 473 nm; λ_{em} = 550-650 nm. Bar = 20 μm.

a)

Dye	Loading conditions	Percentage laser transmission	PMT gain	Offset
SP-14	200 nM / 3 min 100 nM / 10 min 50 nM / 25 min 10 nM / 30 min 5 nM / 30 min 1 nM / 30 min	15%	600	10%

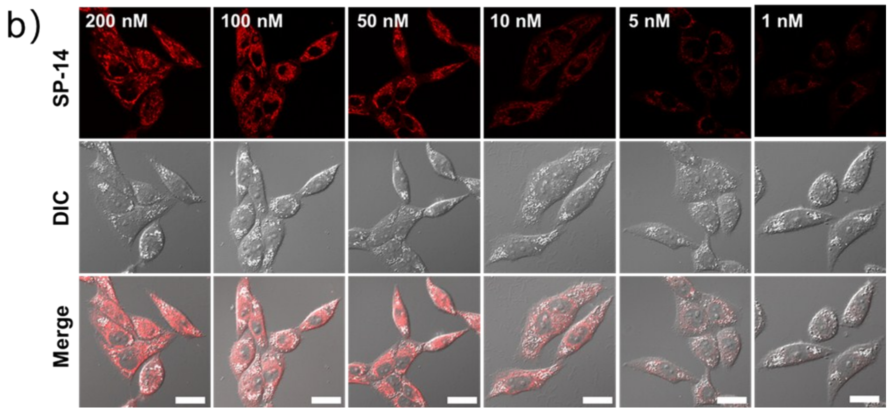

Figure S16. LSCM imaging parameters (a) and images (b) of SiHa cells stained with **SP-10** of different concentrations ranging from 200 nM to 1 nM. λ_{ex} = 473 nm; λ_{em} = 550-650 nm. Bar = 20 μm.

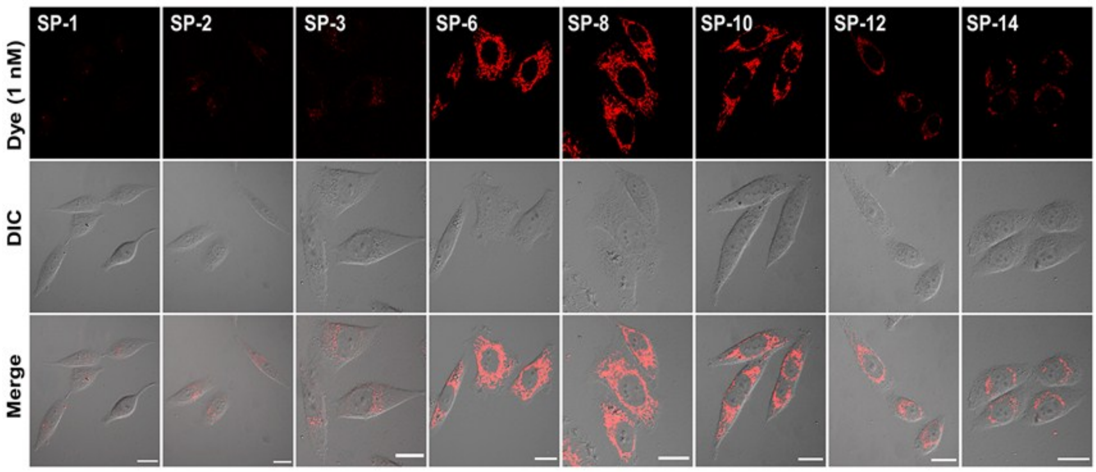

Figure S17. LSCM images of SiHa cells stained with 1 nM **SPs** for 30 min. λ_{ex} = 473 nm; λ_{em} = 550-650 nm. In the experiments, the image acquisition parameters were set to be consistent. Bar = 20 μm.

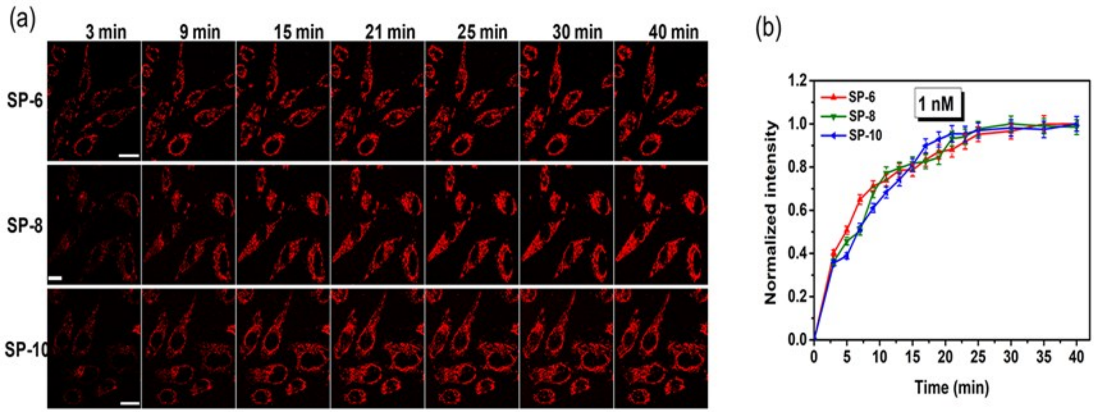

Figure S18. Time-dependent LSCM images (a) of SiHa cells stained with 1 nM **SP-6**, **SP-8**, and **SP-10**, as well as the corresponding normalized fluorescence intensity (b). λ_{ex} = 473 nm; λ_{em} = 550-650 nm. Bar = 20 μm.

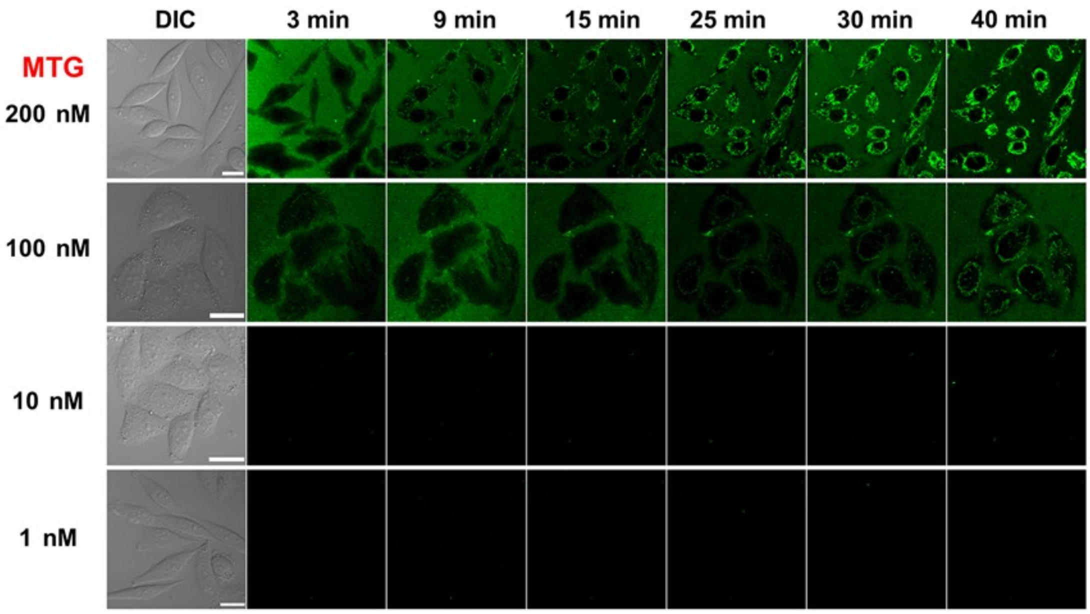

Figure S19. Time-dependent LSCM images of SiHa cells stained with MTG of different concentrations (200 nM, 100 nM, 10 nM, and 1nM). λ_{ex} = 473 nm; λ_{em} = 500-600 nm. Bar = 20 μm.

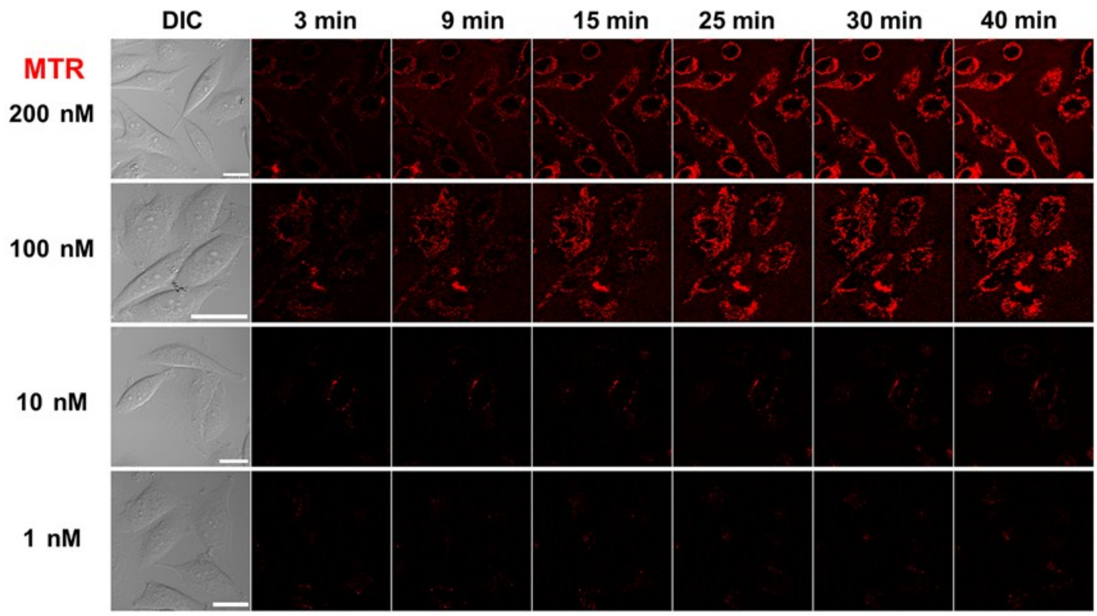

Figure S20. Time-dependent LSCM images of SiHa cells stained with MTR of different concentrations (200 nM, 100 nM, 10 nM, and 1nM). λ_{ex} = 543 nm; λ_{em} = 550-650 nm. Bar = 20 μm.

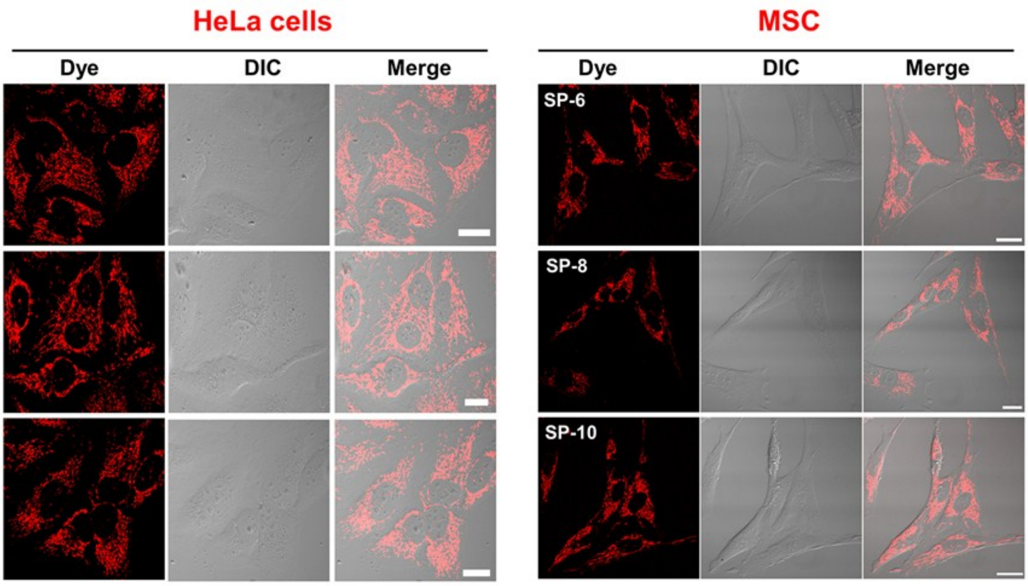

Figure S21. LSCM images of different types of cells (HeLa and MSC) stained with 1 nM **SP-6**, **SP-8**, and **SP-10** for 20 min. λ_{ex} = 473 nm; λ_{em} = 550-650 nm. Bar = 20 μm.

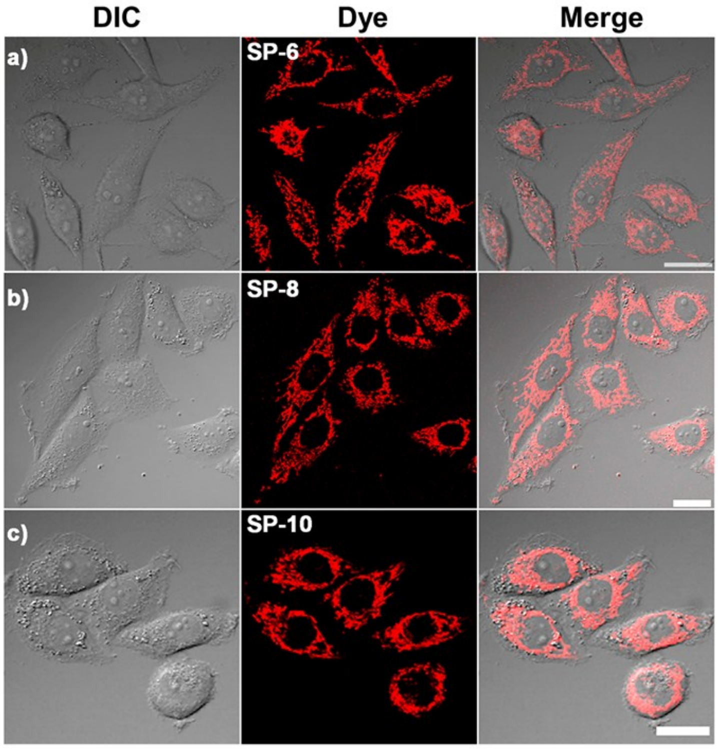

Figure S22. TPEF images of SiHa cells stained with 1 nM **SP-6**, **SP-8**, and **SP-10**. λ_{ex} = 900 nm; λ_{em} = 570-630 nm. Bar = 20 μm.

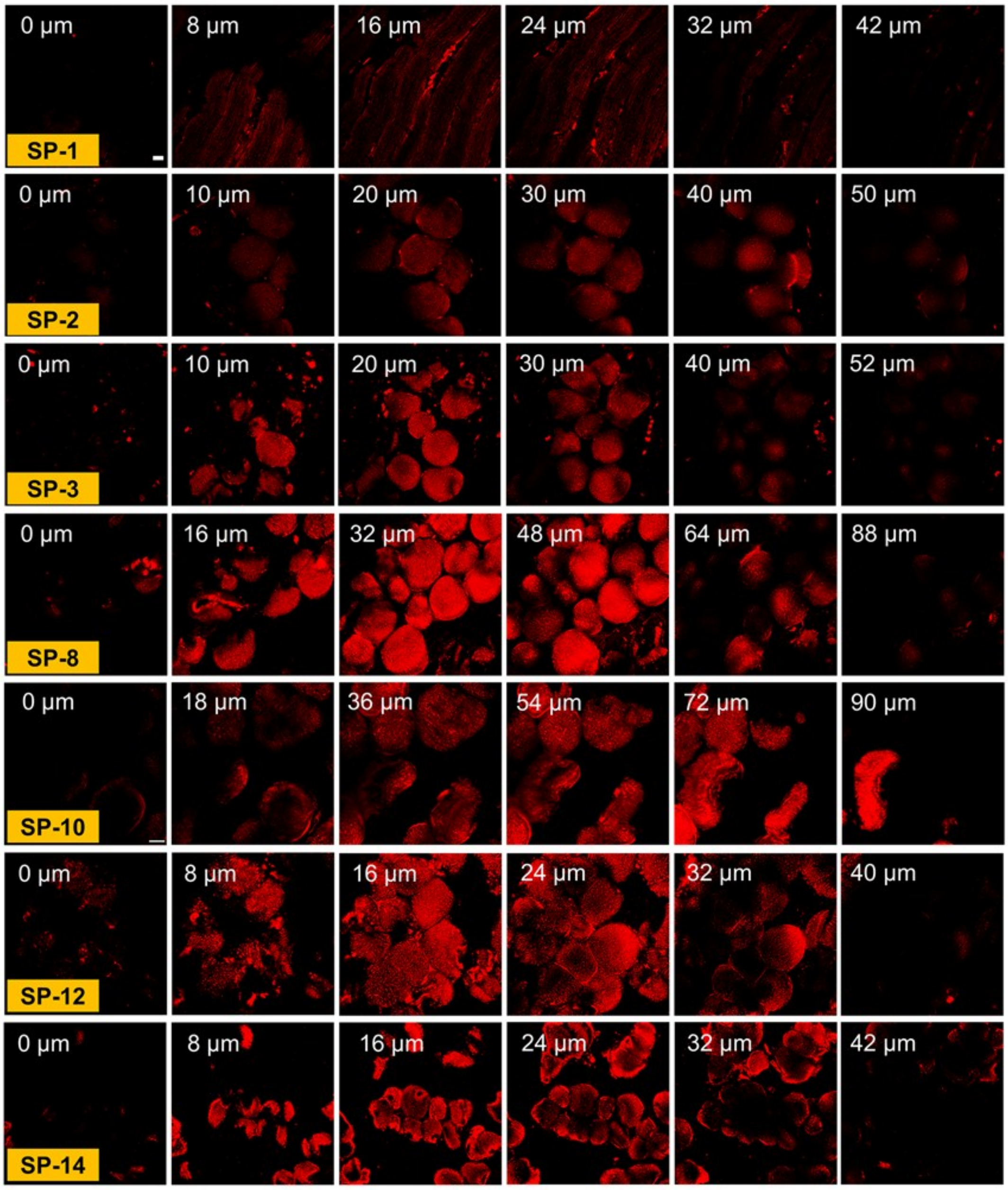

Figure S23. TPEF tomography images at different depths of rat skeletal muscle tissue stained with **SP-1**, **SP-2**, **SP-3**, **SP-8**, **SP-10**, **SP-12**, and **SP-14** (10 μM, 30 min). λ_{ex} = 900 nm, λ_{em} = 570-630 nm. Bar = 20 μm.

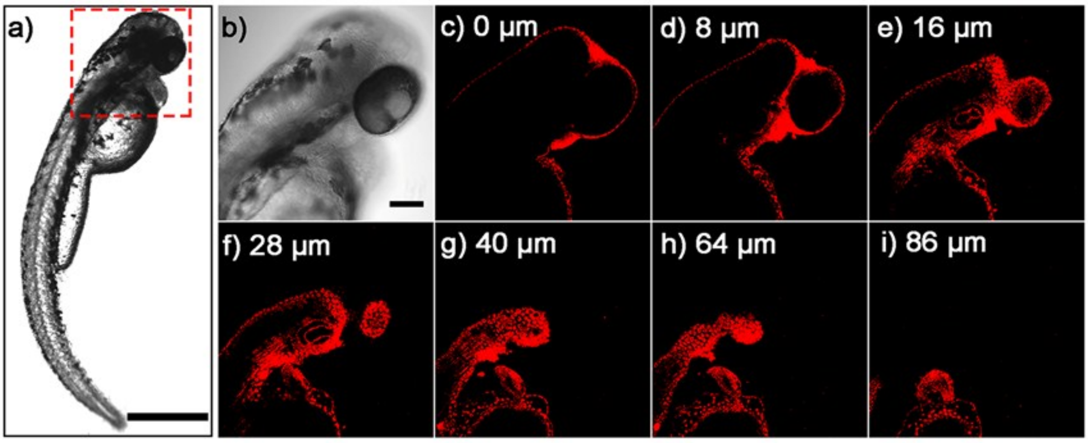

Figure S24. TPEF images of mitochondria in zebrafish stained with **SP-6** (10 μM, 30 min). (a) DIC image, (b) enlargement images of red box in (a), (c-i) tomography images at different depths from 0 μm to 86 μm. λ_{ex} = 900 nm, λ_{em} = 570-630 nm. Bar (a) = 500 μm, bar (b-i) = 100 μm.

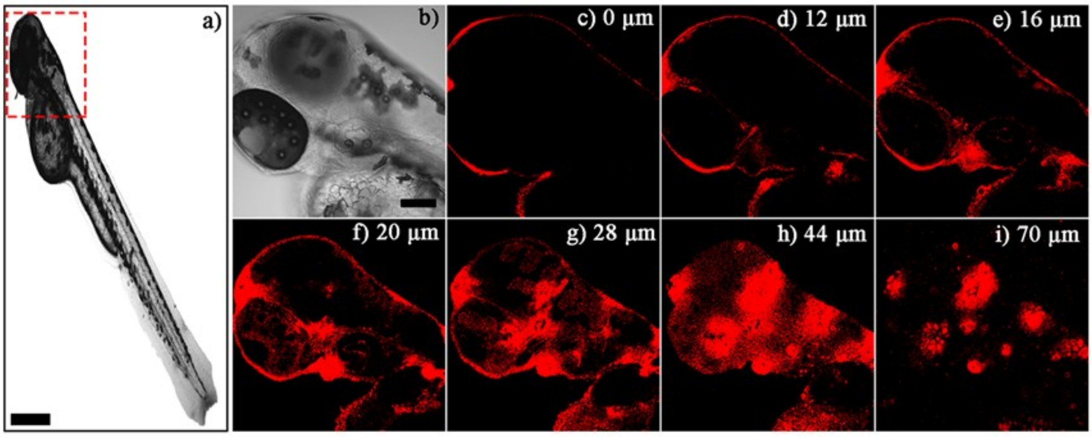

Figure S25. TPEF images of mitochondria in zebrafish stained with **SP-8** (10 μM, 30 min). (a) DIC image, (b) enlargement images of red box in (a), (c-i) tomography images at different depths from 0 μm to 70 μm. λ_{ex} = 900 nm, λ_{em} = 570-630 nm. Bar (a) = 500 μm, bar (b-i) = 100 μm.

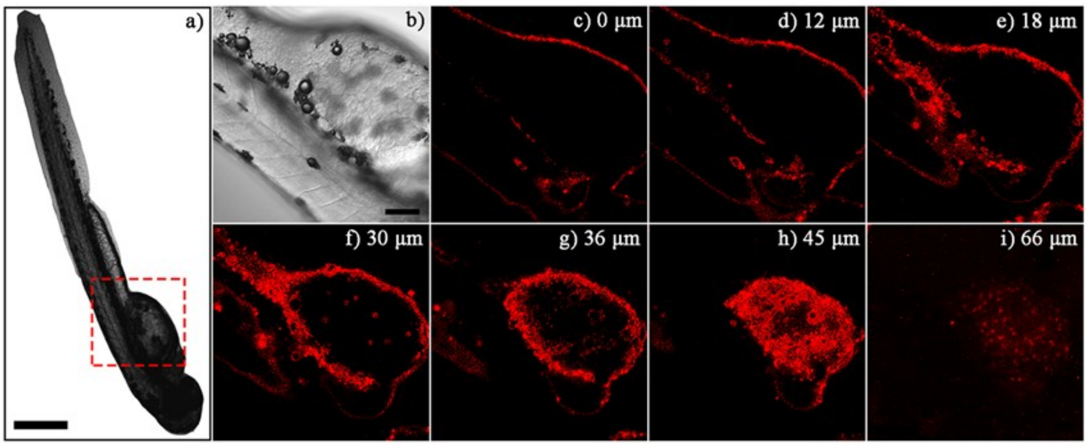

Figure S26. TPEF images of mitochondria in zebrafish stained with **SP-10** (10 μM, 30 min). (a) DIC image, (b) enlargement images of red box in (a), (c-i) tomography images at different depths from 0 μm to 66 μm. λ_{ex} = 900 nm, λ_{em} = 570-630 nm. Bar (a) = 500 μm, bar (b-i) = 100 μm.

Table S2. Optical properties of 9E-BMVC derivatives (**9E-BMVCs**).

Dye	Solvent	λ_{abs}	λ_{em}	$lg\ \varepsilon$	Φ
9E-BMVC1	DMSO	452	557	4.53	0.008
	MeOH	456	558	4.55	0.009
	Gly	460	548	4.55	0.068
9E-BMVC3	DMSO	456	560	4.41	0.011
	MeOH	458	560.5	4.45	0.014
	Gly	462	549.5	4.48	0.064
9E-BMVC6	DMSO	456	563.5	4.46	0.012
	MeOH	458	557	4.50	0.016
	Gly	464	547.5	4.49	0.069
9E-BMVC8	DMSO	456	564	4.51	0.011
	MeOH	460	559.5	4.57	0.014
	Gly	464	551	4.48	0.079
9E-BMVC10	DMSO	456	560	4.61	0.010
	MeOH	460	560	4.65	0.014
	Gly	464	549.5	4.59	0.065
9E-BMVC12	DMSO	456	561.5	4.43	0.012
	MeOH	460	557.5	4.62	0.014
	Gly	464	551	4.59	0.077

λ_{abs}: the maximum emission wavelength, λ_{em}: the maximum emission wavelength (unit: nm); ε: the molar extinction coefficient; Φ: the fluorescence quantum yield. The excitation wavelength: 473 nm.

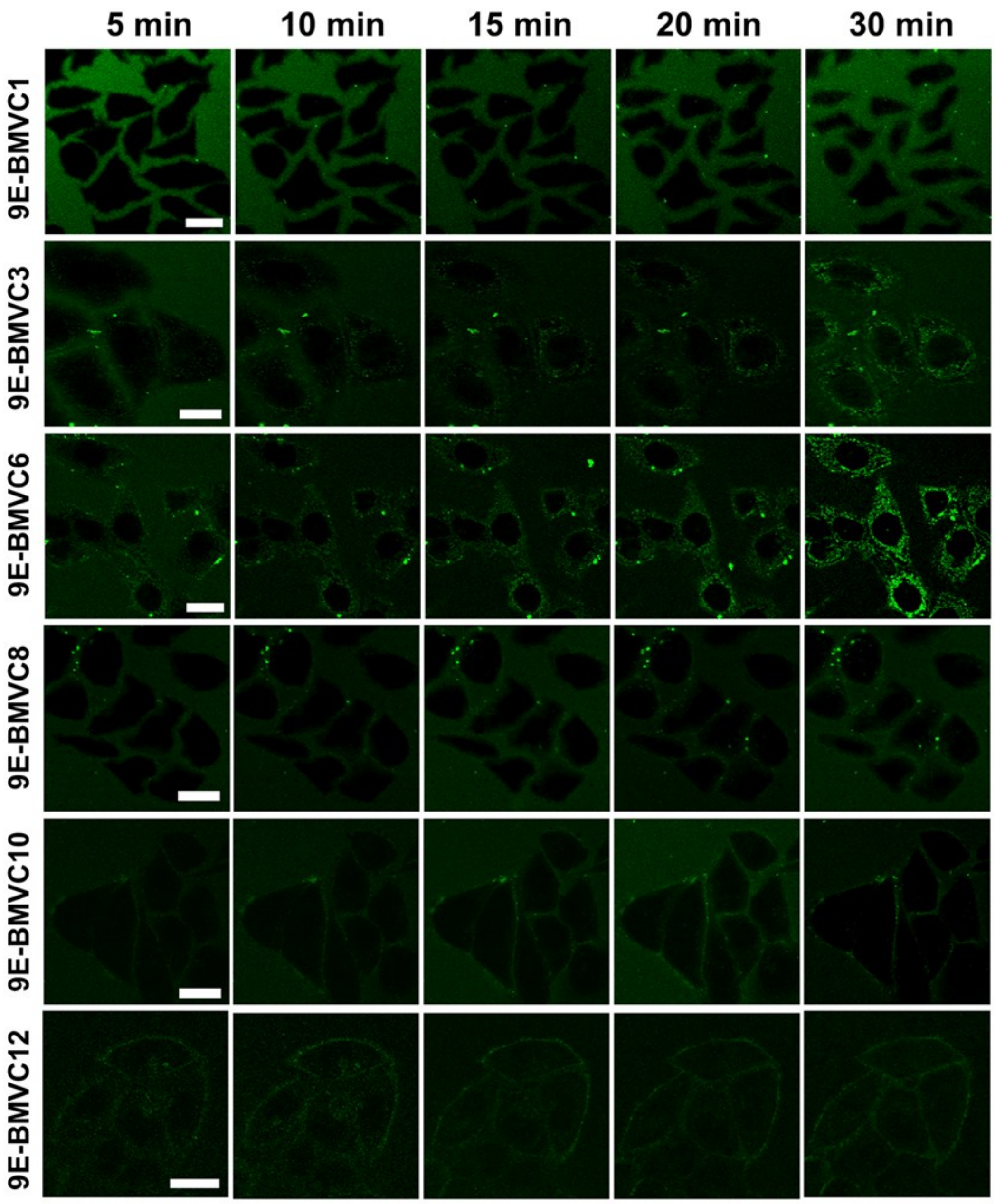

Figure S27. LSCM images of SiHa cells stained with 5 μM **9E-BMVCs** at different time (5-30 min). λ_{ex} = 473 nm, λ_{em} = 500-600 nm. Bar = 20 μm.

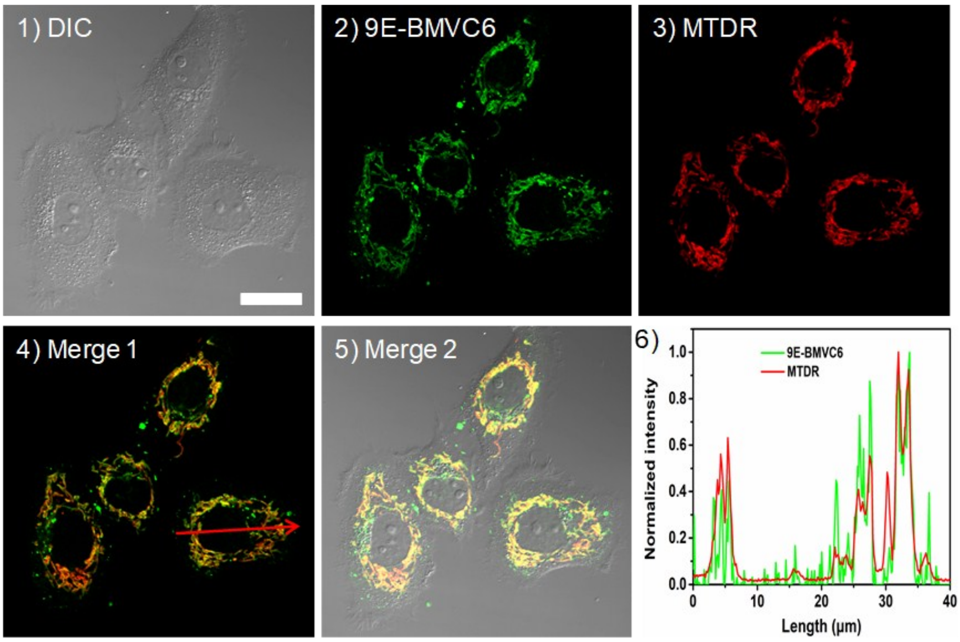

Figure S28. LSCM images of SiHa cells co-stained with **9E-BMVC6** and MTDR. (1): DIC, (2) **9E-BMVC6**, (3) MTDR, (4) merged image of (2) and (3), (5) merged image of (1) - (3), (6) the normalized fluorescence profiles of **9E-BMVC6** and MTDR along the red line in (4). Bar = 20 μm.

Table S3. The ClogP values and the cell permeability of SP derivatives.

Dye	SP-1	SP-2	SP-3	SP-6	SP-8	SP-10	SP-12	SP-14	SP-15	SP-16	SP-18	SP-22
ClogP	-1.34	-0.81	-0.28	1.30	2.36	3.42	4.48	5.53	6.06	6.59	7.65	9.77
Cell permeability	√	√	√	√	√	√	√	√	√	×	×	×

Table S4. The ClogP values and the cell permeability of 9E-BMVC derivatives.

Dye	9E-BMVC1	9E-BMVC3	9E-BMVC6	9E-BMVC8	9E-BMVC10	9E-BMVC12
ClogP	-2.79	-0.14	2.50	4.62	6.74	8.85
Cell permeability	×	√	√	×	×	×

References

1. Xu, C.; Webb, W. W. *J. Opt. Soc. Am. B* **1996**, *13*, 481-491.

2. Albota, M. A.; Xu, C.; Webb, W. W. *Appl. Optics* **1998**, *37*, 7352-7356.

3. Makarov, N. S., Drobizhev, M., Rebane A. *Optical Express*. **2008**, *5*, 4029-4047.

4. (Frisch, M. J.; Trucks, G. W.; Schlegel, H. B.; Scuseria, G. E.; Robb, M. A.; Cheeseman, J. R.; Scalmani, G.; Barone, V.; Men-nucci, B.; Petersson, G. A.; Nakatsuji, H.; Caricato, M.; Li, X.; Hratchian, H. P.; Izmaylov, A. F.; Bloino, J.; Zheng, G.; Son-ne, D. Gaussian 09, revision 1A; Gaussian Inc.: Wallingford, CT, 2009

The synthetic steps and structural characterization of SPs and 9E-BMVC variants.

Scheme S1 The synthesis routine of **SPs**.

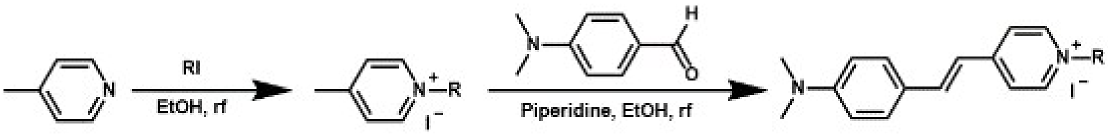

The mixture comprised of 4-methylpyridine (1 mL, 11 mmol) and iodoalkane or bromoalkane (11 mmol) was added into a flask, with ethyl alcohol (5 mL) as the solvent. Next, the reaction system was stirred for 24 h at 85 ^oC. After that, adding 4-(dimethylamino)benzaldehyde (1.53 ml, 11 mmol) and 200uL piperidine into this mixture with stirring at 85 ^oC for 24 h. After being cooled to room temperature, the precipitate was washed with little ethyl alcohol two times and then petroleum ether three times. Red power product was obtained after the residue was recrystallized from ethyl alcohol, with a yield of 80%.

For **SP-1**, ^1H NMR (400 MHz, DMSO-d_6): δ (ppm) 8.68 (d, J = 6.8 Hz, 2H), 8.04 (d, J = 6.8 Hz, 2H), 7.90 (d, J = 16 Hz, 1H), 7.59 (d, J =8.8 Hz, 2H), 7.17 (d, J = 16 Hz, 1H), 6.79 (d, J = 8.8 Hz, 2H), 4.17 (s, 3H), 3.02 (s, 6H). HR-MS calculated for $C_{16}H_{19}N_2^+$ m/z 239.34, found 239.15.

For **SP-2**, ^1H NMR (400 MHz, DMSO-d_6): δ (ppm) 8.79 (d, J = 6.8 Hz, 2H), 8.06 (d, J = 6.8 Hz, 2H), 7.93 (d, J = 16 Hz, 1H), 7.60 (d, J =8.8 Hz, 2H), 7.18 (d, J = 16 Hz, 1H), 6.79 (d, J = 8.8 Hz, 2H), 4.51 (t, J = 2.4 Hz, 2H), 3.02 (s, 6H), 1.50 (t, J = 7.4 Hz, 3H). HR-MS calculated for $C_{17}H_{21}N_2^+$ m/z 253.37, found 253.17.

For **SP-3**, ^1H NMR (400 MHz, DMSO-d_6): δ (ppm) 8.77 (d, J = 6.8 Hz, 2H), 8.07 (d, J = 7.2 Hz, 2H), 7.93 (d, J = 16 Hz, 1H), 7.60 (d, J =9.2 Hz, 2H), 7.18 (d, J = 16 Hz, 1H), 6.79 (d, J = 8.8 Hz, 2H), 4.39 (t, J = 7.4 Hz, 2H), 3.02 (s, 6H), 1.90 (q, J = 7.3 Hz, 2H), 0.89 (t, J = 7.2 Hz, 3H). HR-MS calculated for $C_{18}H_{23}N_2^+$ m/z 267.40, found 267.19.

For **SP-6**, ^1H NMR (400 MHz, DMSO-d_6): δ (ppm) 8.78 (d, J = 6.8 Hz, 2H), 8.08 (d, J = 6.8 Hz, 2H), 7.95 (d, J = 16.0 Hz, 1H), 7.61 (d, J = 8.8 Hz, 2H), 7.19 (d, J = 16.4 Hz, 1H), 6.79 (d, J = 8.8 Hz, 2H), 4.42 (t, J = 7.2 Hz, 2H), 3.03 (s, 6H), 1.88 (t, J = 6.6 Hz, 2H), 1.28 (s, 6H), 0.86 (t, J = 6.8 Hz, 3H). HR-MS calculated for

$C_{21}H_{29}N_2^+$ m/z 309.48, found 309.23.

For **SP-8**, ^{1}H NMR (400 MHz, DMSO-d_6): δ (ppm) 8.78 (d, J = 6.8 Hz, 2H), 8.07 (d, J = 6.8 Hz, 2H), 7.94 (d, J = 16.0 Hz, 1H), 7.60 (d, J =9.2 Hz, 2H), 7.19 (d, J = 16.4 Hz, 1H), 6.79 (d, J = 8.8 Hz, 2H), 4.41 (t, J = 7.2 Hz, 2H), 3.03 (s, 6H), 1.89 (t, J = 6.4 Hz, 2H), 1.26 (s, 10H), 0.86 (t, J = 6.8 Hz, 3H). HR-MS calculated for $C_{23}H_{33}N_2^+$ m/z 337.53, found 337.27.

For **SP-10**, ^{1}H NMR (300 MHz, DMSO-d_6): δ (ppm) 8.78 (d, J = 6.9 Hz, 2H), 8.07 (d, J = 6.8 Hz, 2H), 7.94 (d, J = 16.0 Hz, 1H), 7.60 (d, J = 9.2 Hz, 2H), 7.19 (d, J = 16.0 Hz, 1H), 6.79 (d, J = 9.2 Hz, 2H), 4.41 (t, J = 7.4 Hz, 2H), 3.03 (s, 6H), 1.88 (t, J = 6.6 Hz, 2H), 1.27 (s, 14H), 0.85 (t, J = 7.0 Hz, 3H). HR-MS calculated for $C_{25}H_{37}N_2^+$ m/z 365.58, found 365.30.

For **SP-12**, ^{1}H NMR (400 MHz, DMSO-d_6): δ (ppm) 8.78 (d, J = 6.8 Hz, 2H), 8.07 (d, J = 6.8 Hz, 2H), 7.94 (d, J = 16.0 Hz, 1H), 7.60 (d, J = 8.8 Hz, 2H), 7.18 (d, J = 16.0 Hz, 1H), 6.80 (d, J = 9.2 Hz, 2H), 4.41 (t, J = 7.4 Hz, 2H), 3.03 (s, 6H), 1.88 (t, J = 6.6 Hz, 2H), 1.25 (s, 18H), 0.85 (t, J = 6.8 Hz, 3H). HR-MS calculated for $C_{27}H_{41}N_2^+$ m/z 393.64, found 393.33.

For **SP-14**, ^{1}H NMR (400 MHz, DMSO-d_6): δ (ppm) 8.79 (d, J = 6.8 Hz, 2H), 8.07 (d, J = 6.8 Hz, 2H), 7.94 (d, J = 16 Hz, 1H), 7.60 (d, J = 9.2 Hz, 2H), 7.18 (d, J = 16 Hz, 1H), 6.80 (d, J = 8.8 Hz, 2H), 4.41 (t, J = 7.2 Hz, 2H), 3.03 (s, 6H), 1.88 (t, J = 6.4 Hz, 2H), 1.25 (s, 22H), 0.85 (t, J = 6.8 Hz, 3H). HR-MS calculated for $C_{29}H_{45}N_2^+$ m/z 421.69, found 421.36.

For **SP-15**, ^{1}H NMR (400 MHz, DMSO-d_6): δ (ppm) 8.78 (d, J = 6.8 Hz, 2H), 8.07 (d, J = 6.8 Hz, 2H), 7.93 (d, J = 16.4 Hz, 1H), 7.60 (d, J = 8.8 Hz, 2H), 7.18 (d, J = 16 Hz, 1H), 6.79 (d, J = 9.2 Hz, 2H), 4.41 (t, J = 7.4 Hz, 2H), 3.03 (s, 6H), 1.87 (t, J = 6.4 Hz 2H), 1.22 (s, 24H), 0.85 (t, J = 6.8 Hz, 3H). HR-MS calculated for $C_{30}H_{47}N_2^+$ m/z 435.72, found 435.37.

For **SP-16**, ^{1}H NMR (400 MHz, DMSO-d_6): δ (ppm) 8.78 (d, J = 6.8 Hz, 2H), 8.07 (d, J = 6.8 Hz, 2H), 7.94 (d, J = 16.0 Hz, 1H), 7.60 (d, J = 9.2 Hz, 2H), 7.18 (d, J = 16.0 Hz, 1H), 6.80 (d, J = 9.2 Hz, 2H), 4.41 (t, J = 7.2 Hz, 2H), 3.03 (s, 6H), 1.88 (t, J = 6.6 Hz, 2H), 1.24 (s, 26H), 0.85 (t, J = 7.0 Hz, 3H). HR-MS calculated for

$C_{30}H_{47}N_2^+$ m/z 449.75, found 449.39.

For **SP-18**, ^{1}H NMR (400 MHz, DMSO-d_6): δ (ppm) 8.77 (d, J = 6.8 Hz, 2H), 8.06 (d, J = 7.2 Hz, 2H), 7.92 (d, J = 16.4 Hz, 1H), 7.60 (d, J = 9.2 Hz, 2H), 7.17 (d, J = 16.0 Hz, 1H), 6.79 (d, J = 8.8 Hz, 2H), 4.40 (t, 2H), 3.04 (s, 6H), 1.88 (t, J = 6.4 Hz, 2H), 1.25 (s, 32H), 0.85 (t, J = 6.8 Hz, 3H). HR-MS calculated for $C_{33}H_{53}N_2^+$ m/z 477.80, found 477.42.

For **SP-22**, ^{1}H NMR (400 MHz, DMSO-d_6): δ (ppm) δ (ppm) 8.77 (d, J = 6.8 Hz, 2H), 8.06 (d, J = 6.8 Hz, 2H), 7.92 (d, J = 16.0 Hz, 1H), 7.60 (d, J = 8.8 Hz, 2H), 7.17 (d, J = 16.4 Hz, 1H), 6.79 (d, J = 8.8 Hz, 2H), 4.40 (t, J = 14.4 Hz, 2H), 3.04 (s, 6H), 1.87 (t, J = 6.8 Hz, 2H), 1.25 (s, 40H), 0.85 (t, J = 6.8 Hz, 3H). HR-MS calculated for $C_{37}H_{61}N_2^+$ m/z 533.91, found 533.48.

Scheme S2 The synthesis routine of **9E-BMVCs**.

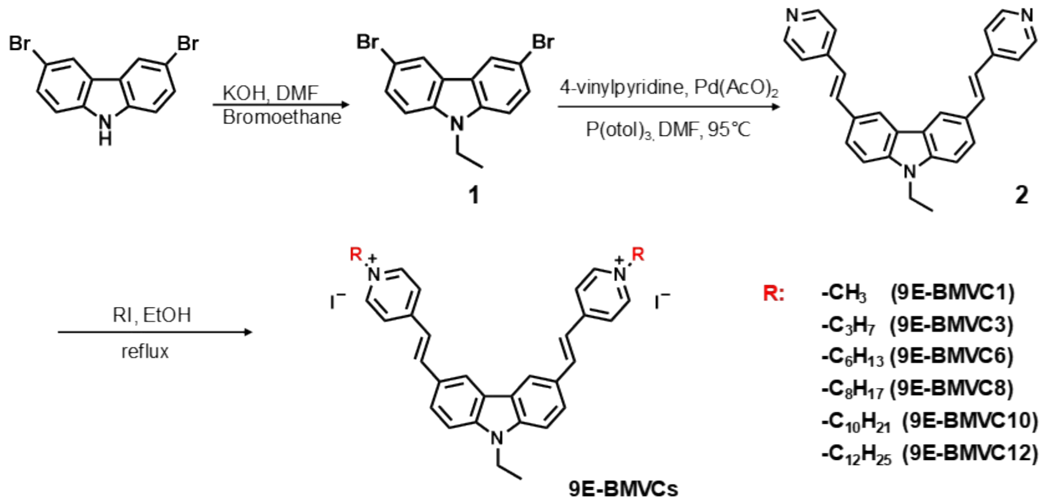

3,6-dibromo-9-(2-ethyl)-carbazole (1): 3 g KOH was initially added into a 250 mL flask, then 30 mL DMF was slowly poured in. After that the mixture has been stirred up to 10 min, 2 g 3,6- Dibromo-9H-carbazole was carefully added. Then the mixture was stirred for 30 min, and 1.38 mL (12.3 mmol) bromoethane was subsequently added. The resulting system was then stirred for over 18 h to finish the reaction at room temperature. After that, the reaction solution was poured into 400 mL water and then extracted with 400 mL dichloromethane. The organic compartment was then dried with 4 g anhydrous Na_2SO4. Further removing of the solvents could give the final products of white powder, and the yield is 83%. ^{1}H NMR (400 MHz, DMSO-*d6*) δ 8.48 (dd, *J* = 1.8, 0.7 Hz, 2H), 7.62 (m, 4H), 4.44 (q, *J* = 7.1 Hz, 2H), 1.28 (t, *J* = 7.1 Hz, 3H).

9-(2-ethyl)-3,6-bis((E)-2-(pyridin-4-yl)vinyl)-carbazole (2): 1 g (2.83 mmol) of compound 1, 0.0283 g (0.126 mmol) of palladium acetate and 0.115 g (0.378 mmol) of tri(o-tolyl)phosphine were firstly added into a three-necked flask. Then, 20 mL DMF was added to the flask, and the system was subsequently stirred for 5 min before the addition of 5 mL trimethylamine and 1.08 mL (10.1 mmol) 4-vinyl pyridine. The solution was then stirred and bubbled with nitrogen for more than 30 min. The system was consequently heated to 95℃ and stirred for at least 48 h under the protection of nitrogen to complete the reaction. The reaction solution was then poured into 400 mL water and then extracted with 400 mL dichloromethane. The organic compartment was then dried with 4 g anhydrous Na_2SO4. The final products were purified with column chromatography separation method as yellow powder, and the yield is 60%. ^{1}H NMR (300 MHz, DMSO-*d6*) δ 8.55 (d, *J* = 6.0 Hz, 4H), 8.52 (s, 2H), 7.84 (d, *J* = 1.5 Hz, 2H), 7.76 (m, 4H), 7.59 (t, *J* = 6.0 Hz, 4H), 7.28 (d, *J* = 16.5 Hz, 2H), 4.50 (q, *J* = 7.0 Hz, 2H), 1.35 (t, *J* = 6.9 Hz, 3H).

9-(2-ethyl)-3,7-bis(1-methyl-4-pyridinium) carbazole diiodide (9E-BHVC1): 0.2 g (0.499 mmol) of compound 2 was firstly added into a three-necked flask with 20 mL ethanol. The mixture was then stirred evenly before the addition of 2.5mmol RI. The solution was then stirred for more than 10 min and heated to 80 ℃. The reaction was finished for at least 36 h when red powder was precipitated. Then the solution was cooled down to room temperature and filtered, the solids was washed with ethanol for three times as crude product. The final product was further purified by recrystallization in ethanol as red powder, and the yield was 82%. The synthesis routes of other **9E-BHVCs** were similar.

For **9E-BMVC1**, ^{1}H NMR (400 MHz, DMSO-d_6) δ (ppm) 8.84 (d, *J* = 6.6 Hz, 4H), 8.63 (s, 2H), 8.23 (m, 6H), 7.97 (dd, *J* = 8.6, 1.7 Hz, 2H), 7.82 (d, *J* = 8.7 Hz, 2H), 7.58 (d, *J* = 16.2 Hz, 2H), 4.55 (q, *J* = 7.0 Hz, 2H), 4.26 (s, 6H), 1.38 (t, *J* = 7.1 Hz, 3H). HR-MS calculated for $C_{30}H_{29}N_3^{2+}$ m/z 215.79, found 215.62.

For **9E-BMVC3**, ^{1}H NMR (400 MHz, DMSO-d_6) δ (ppm) 8.93 (d, J = 6.7 Hz, 4H), 8.63 (s, 2H), 8.26 (m, 6H), 7.98 (dd, J = 8.7, 1.7 Hz, 2H), 7.84 (d, J = 8.6 Hz, 2H), 7.59 (d, J = 16.2 Hz, 2H), 4.60 (m, 2H), 4.47 (d, J = 7.3 Hz, 4H), 1.96 (t, J = 7.3 Hz, 4H), 1.39 (t, J = 7.1 Hz, 3H), 0.93 (t, J = 7.4 Hz, 6H). HR-MS calculated for $C_{34}H_{37}N_3^{2+}$ m/z 243.84, found 243.65.

For **9E-BMVC6**, ^{1}H NMR (400 MHz, DMSO-d_6) δ (ppm) 8.93 (d, J = 6.7 Hz, 4H), 8.63 (s, 2H), 8.26 (m, 6H), 7.98 (dd, J = 8.7, 1.7 Hz, 2H), 7.84 (d, J = 8.8 Hz, 2H), 7.58 (d, J = 16.4 Hz, 2H), 4.50 (m, 6H), 1.93 (t, J = 7.3 Hz, 4H), 1.39 (t, J = 7.1 Hz, 3H), 1.31 (s, 12H), 0.87 (m, 6H). HR-MS calculated for $C_{40}H_{49}N_3^{2+}$ m/z 285.92, found 285.71.

For **9E-BMVC8**, ^{1}H NMR (400 MHz, DMSO-d_6) δ (ppm) 8.94 (d, J = 6.6 Hz, 4H), 8.64 (s, 2H), 8.25 (m, 6H), 7.98 (dd, J = 8.7, 1.7 Hz, 2H), 7.83 (d, J = 8.7 Hz, 2H), 7.59 (d, J = 16.2 Hz, 4H), 4.50 (m, 6H), 1.92 (t, J = 7.2 Hz, 4H), 1.38 (t, J = 7.1 Hz, 3H), 1.29 (m, 20H), 0.88 (m, 6H). HR-MS calculated for $C_{44}H_{57}N_3^{2+}$ m/z 313.98, found 313.99.

For **9E-BMVC10**, ^{1}H NMR (400 MHz, DMSO-d_6) δ (ppm) 8.94 (d, J = 6.6 Hz, 4H), 8.63 (s, 2H), 8.26 (m, 6H), 7.98 (dd, J = 8.7, 1.6 Hz, 1H), 7.84 (d, J = 8.7 Hz, 2H), 7.59 (d, J = 16.2 Hz, 2H), 4.52(m, 6H), 1.93 (d, J = 8.0 Hz, 4H), 1.39 (t, J = 7.1 Hz, 3H), 1.30 (m, 28H), 0.8 (m, 6H). HR-MS calculated for $C_{48}H_{65}N_3^{2+}$ m/z 342.03, found 341.78.

For **9E-BMVC12**, ^{1}H NMR (400 MHz, DMSO-d_6) δ (ppm) 8.93 (d, J = 6.6 Hz, 4H), 8.63 (s, 2H), 8.23 (m, 6H), 7.97 (dd, J = 8.7, 1.6 Hz, 2H), 7.83 (d, J = 8.7 Hz, 2H), 7.59 (d, J = 16.1 Hz, 2H), 4.50 (m, 6H), 1.92 (t, J = 7.1 Hz, 4H), 1.38 (t, J = 7.2 Hz, 3H), 1.29 (m, 36H), 0.84 (m, 6H). HR-MS calculated for $C_{52}H_{73}N_3^{2+}$ m/z 370.09, found 369.83.

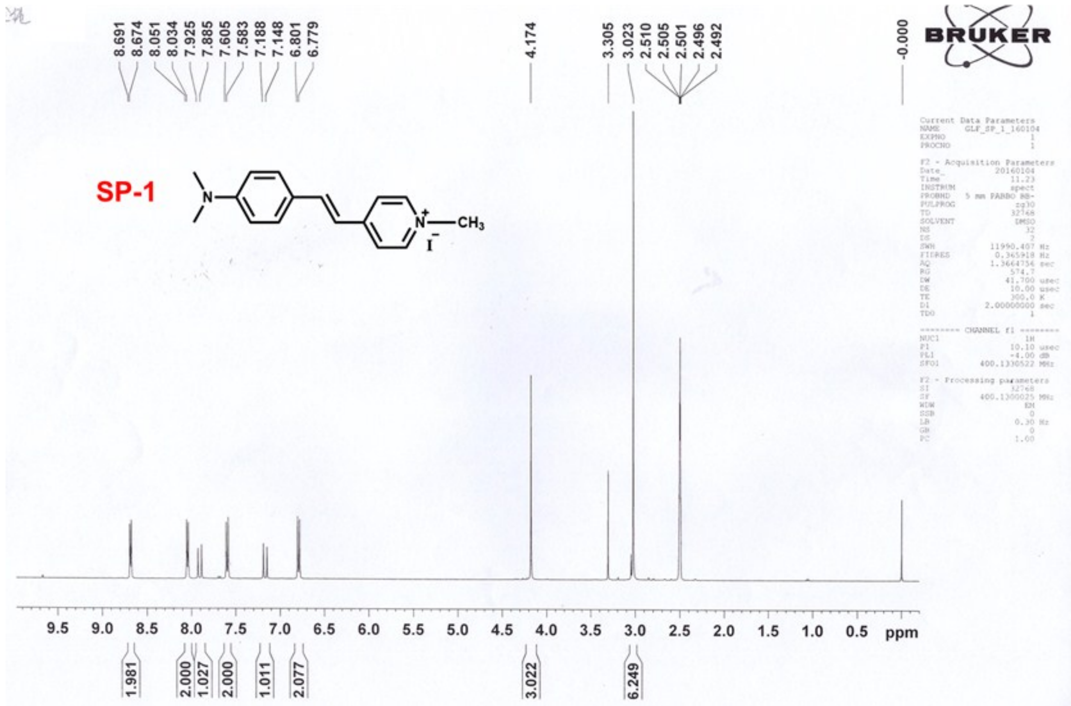

[1]H NMR spectrum of **SP-1** in DMSO-d_6.

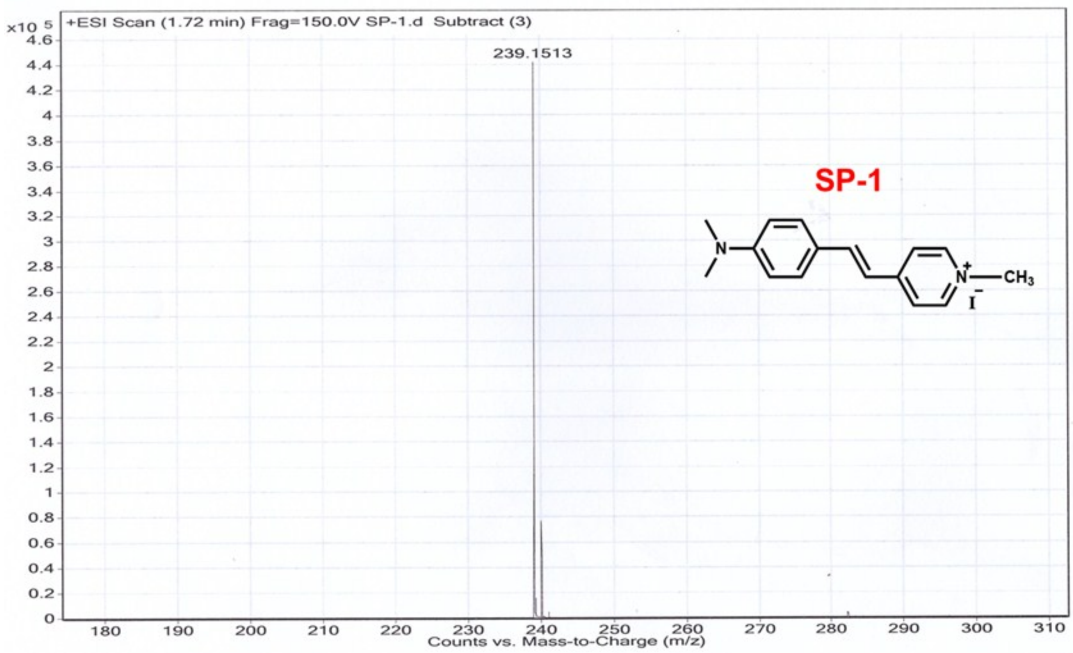

HRMS spectrum of **SP-1** in MeOH.

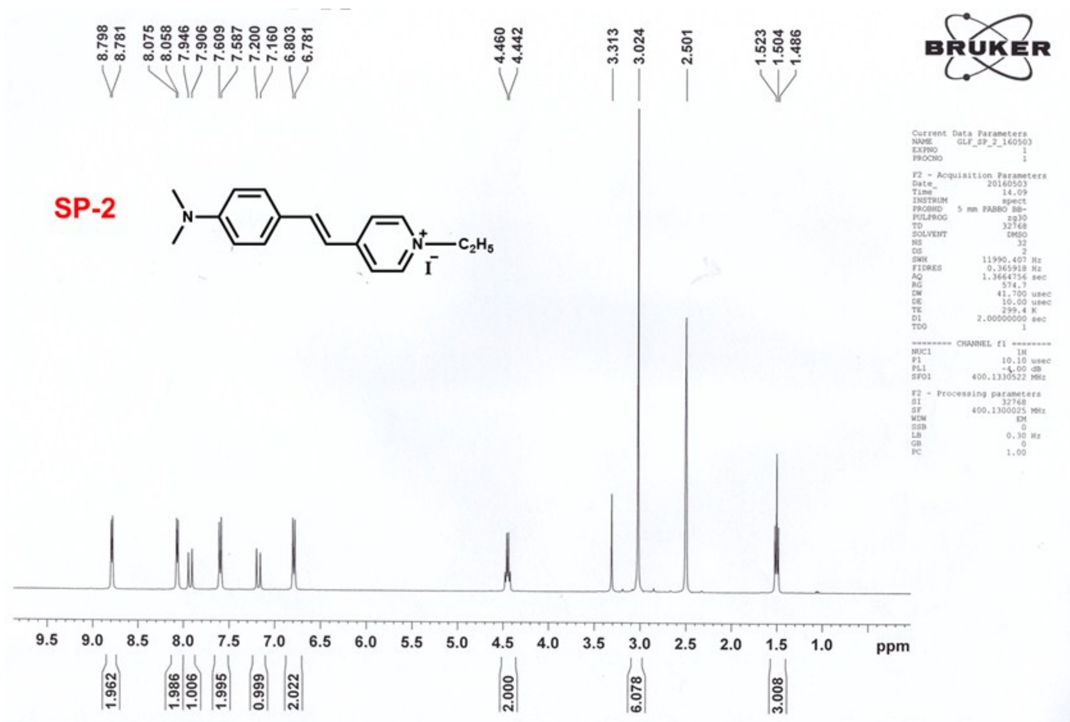

^{1}H NMR spectrum of **SP-2** in DMSO-d_6.

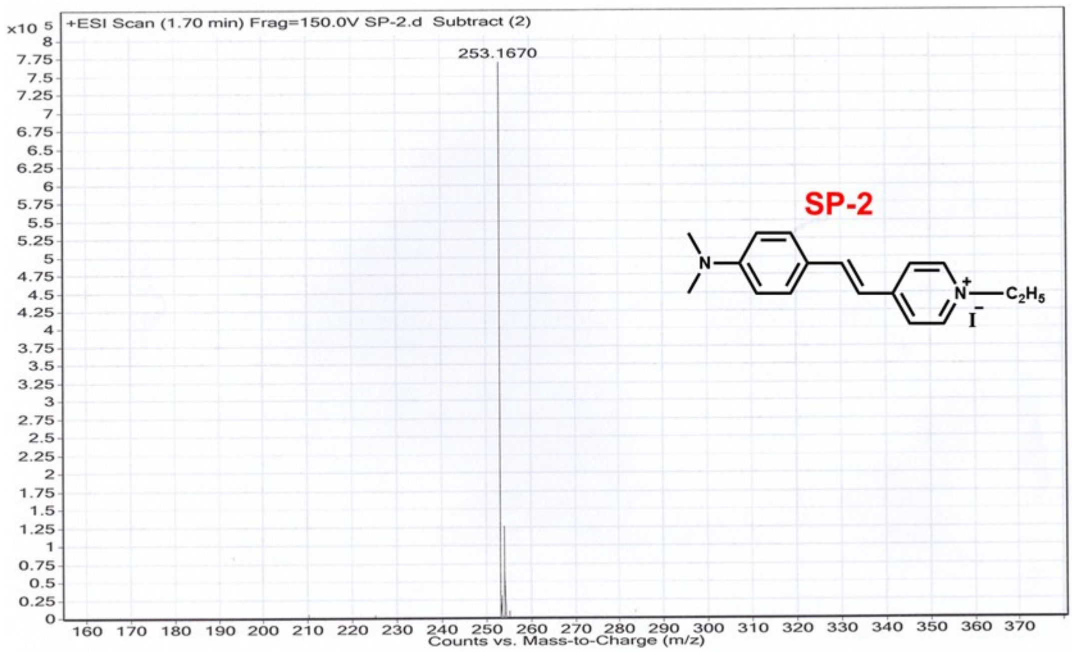

HRMS spectrum of **SP-2** in MeOH.

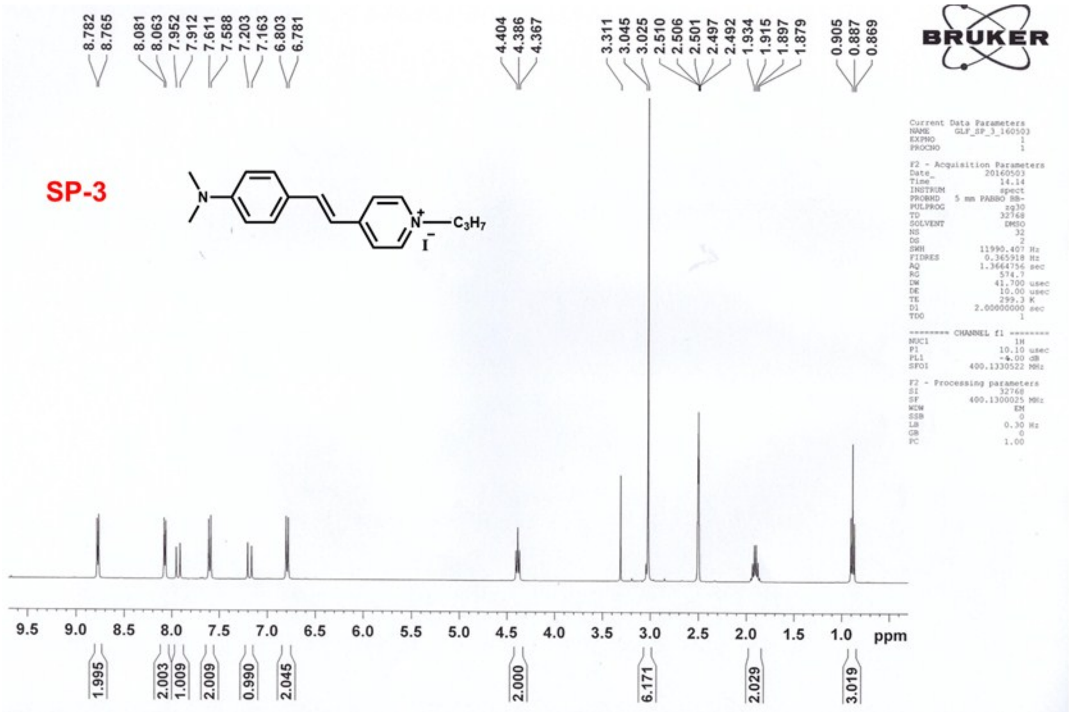

^{1}H NMR spectrum of **SP-3** in DMSO-d_6.

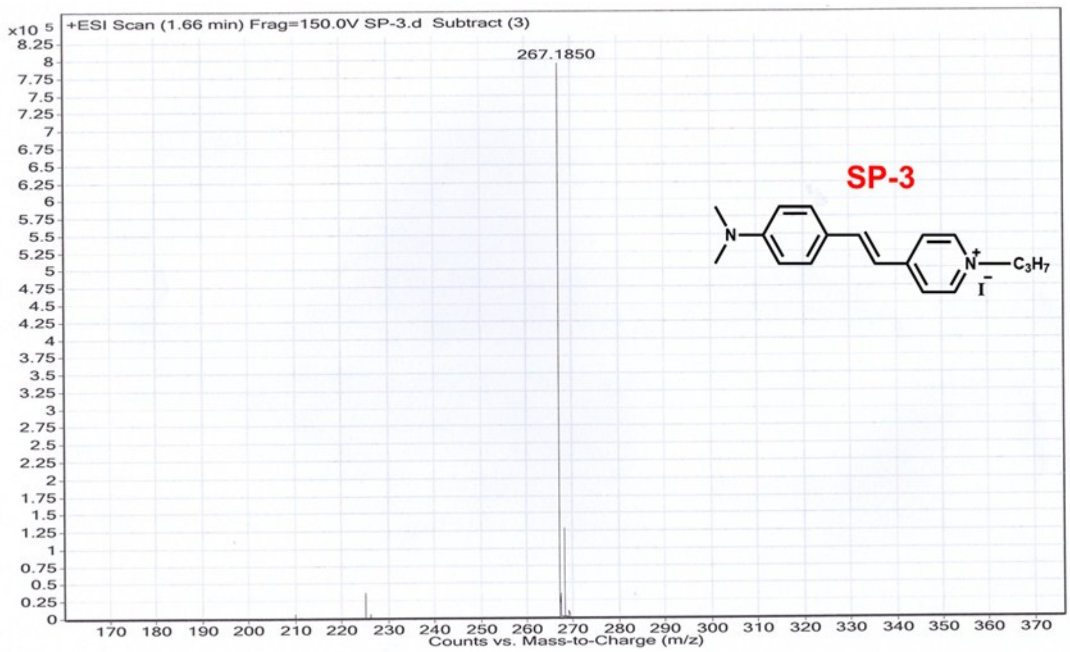

HRMS spectrum of **SP-3** in MeOH.

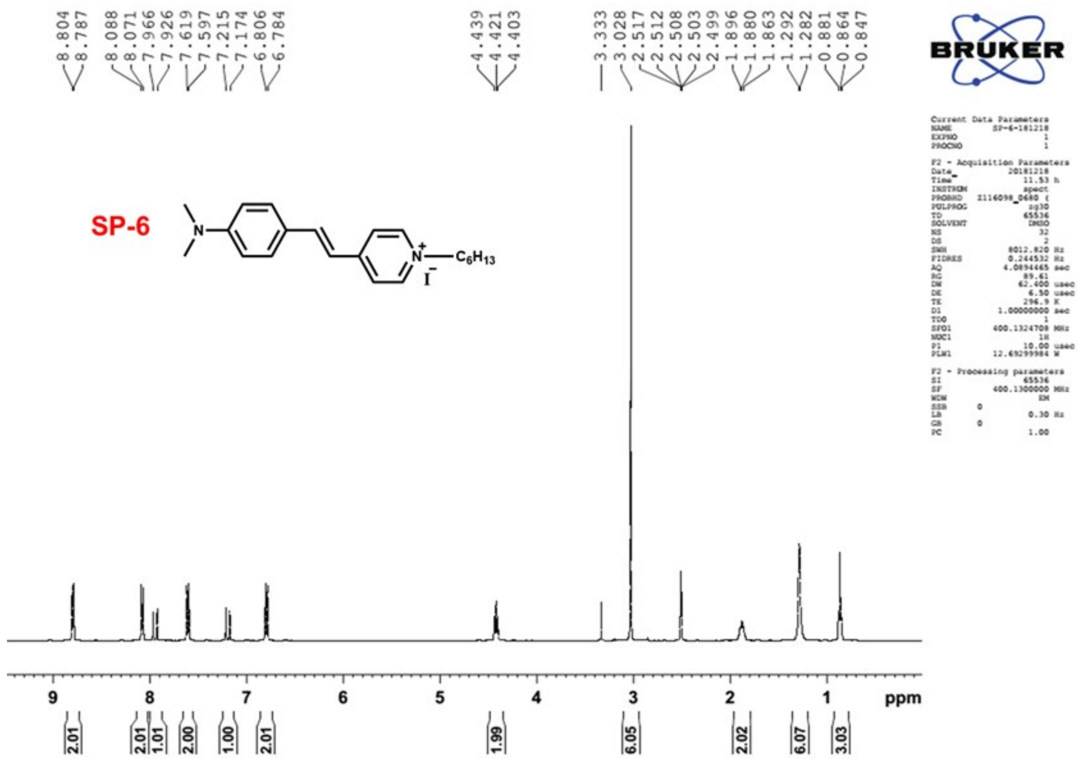

^{1}H NMR spectrum of **SP-6** in DMSO-d_6.

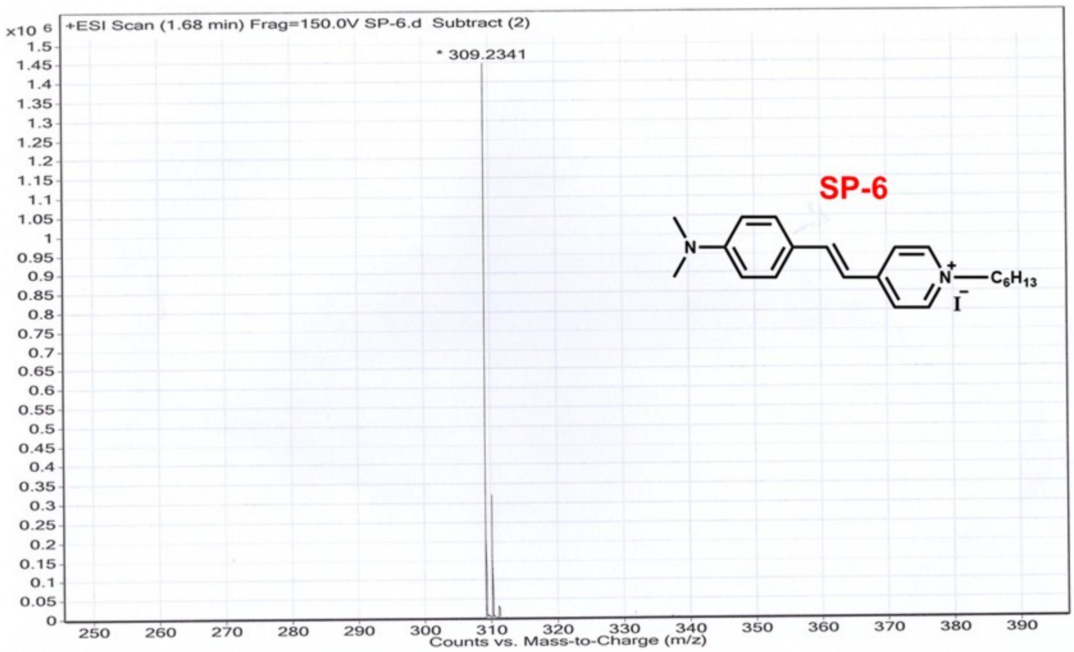

HRMS spectrum of **SP-6** in MeOH.

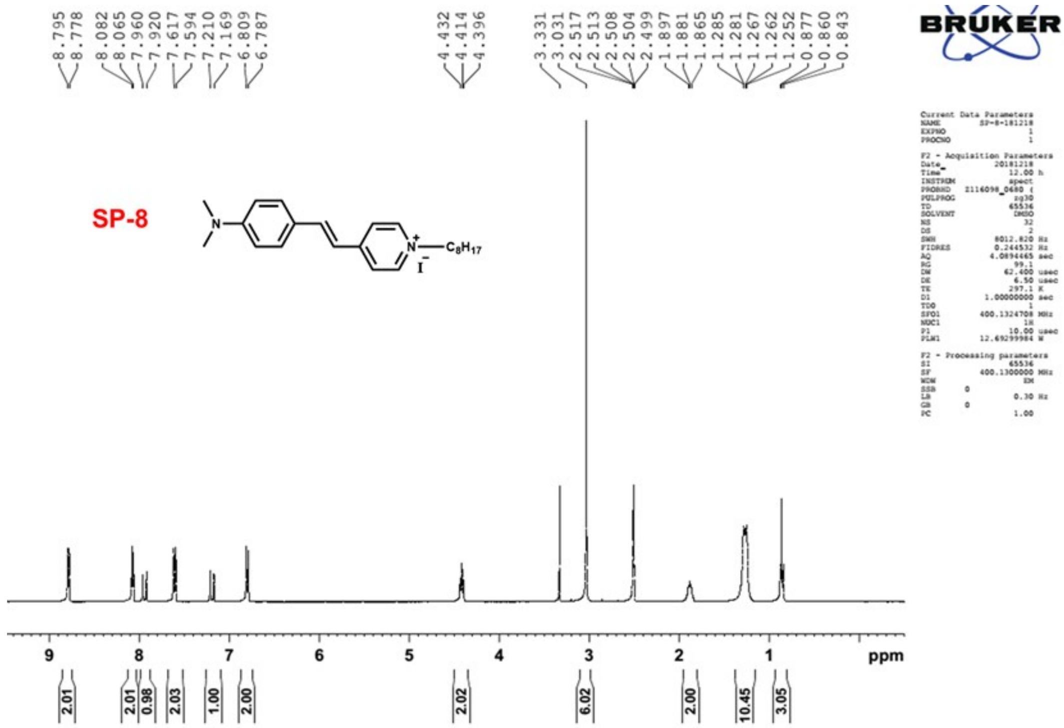

[1]H NMR spectrum of **SP-8** in DMSO-d_6.

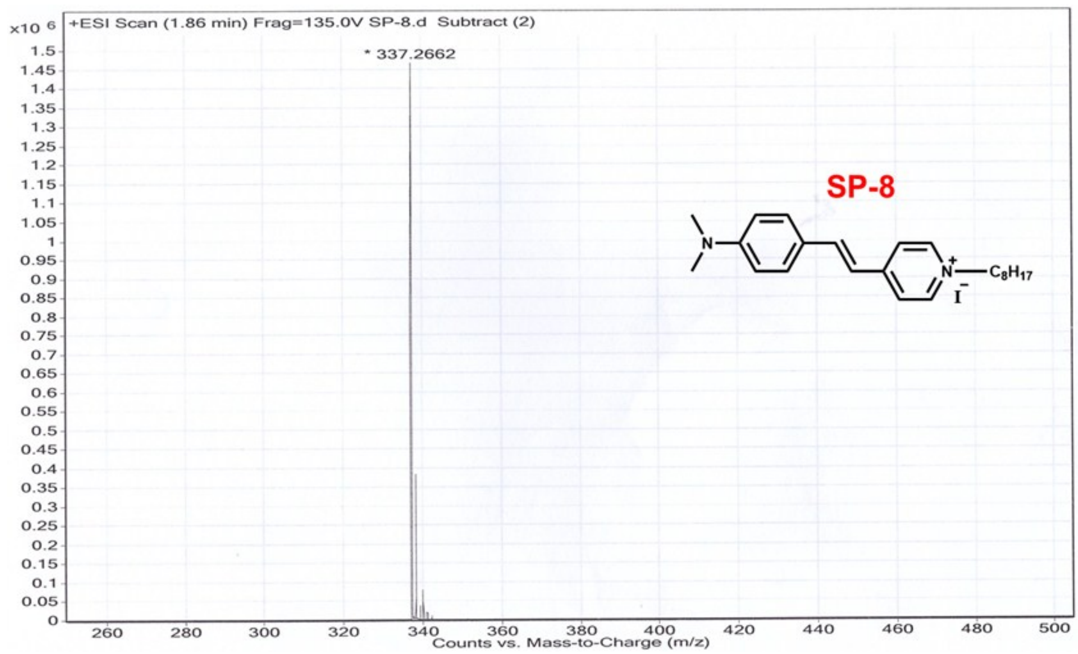

HRMS spectrum of **SP-6** in MeOH.

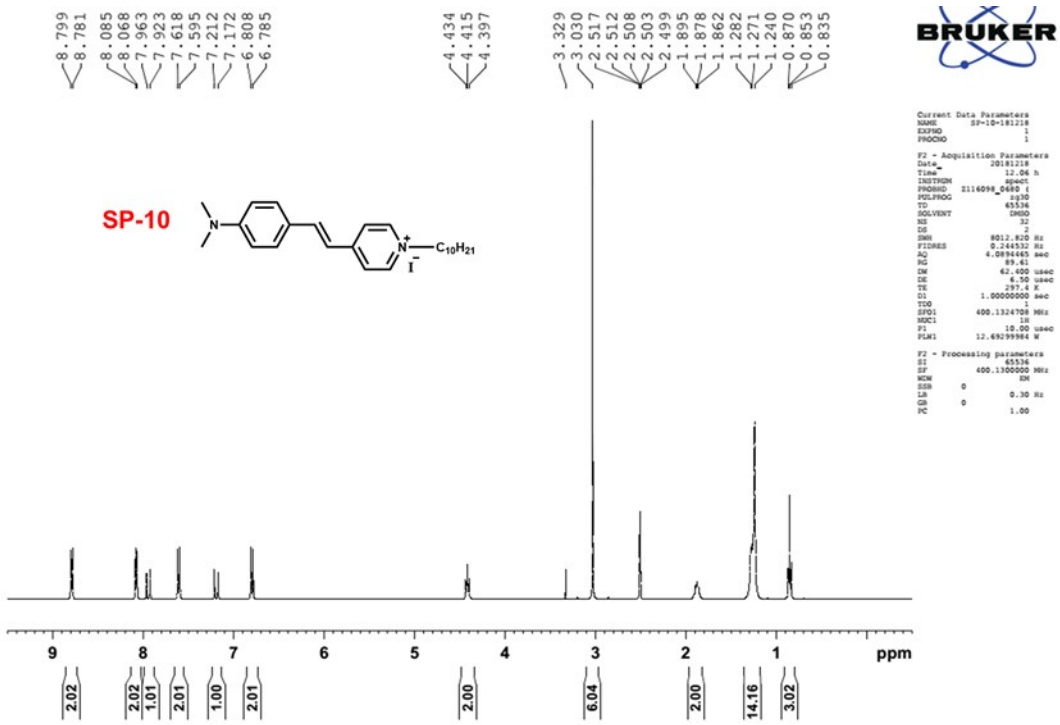

[1]H NMR spectrum of **SP-10** in DMSO-d_6.

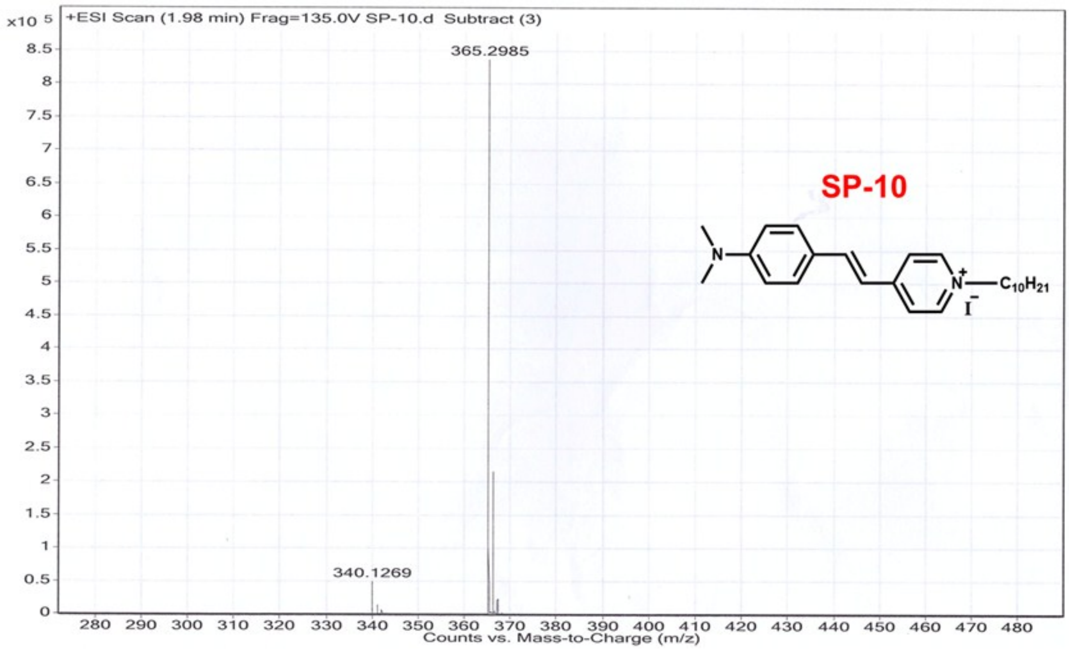

HRMS spectrum of **SP-10** in MeOH.

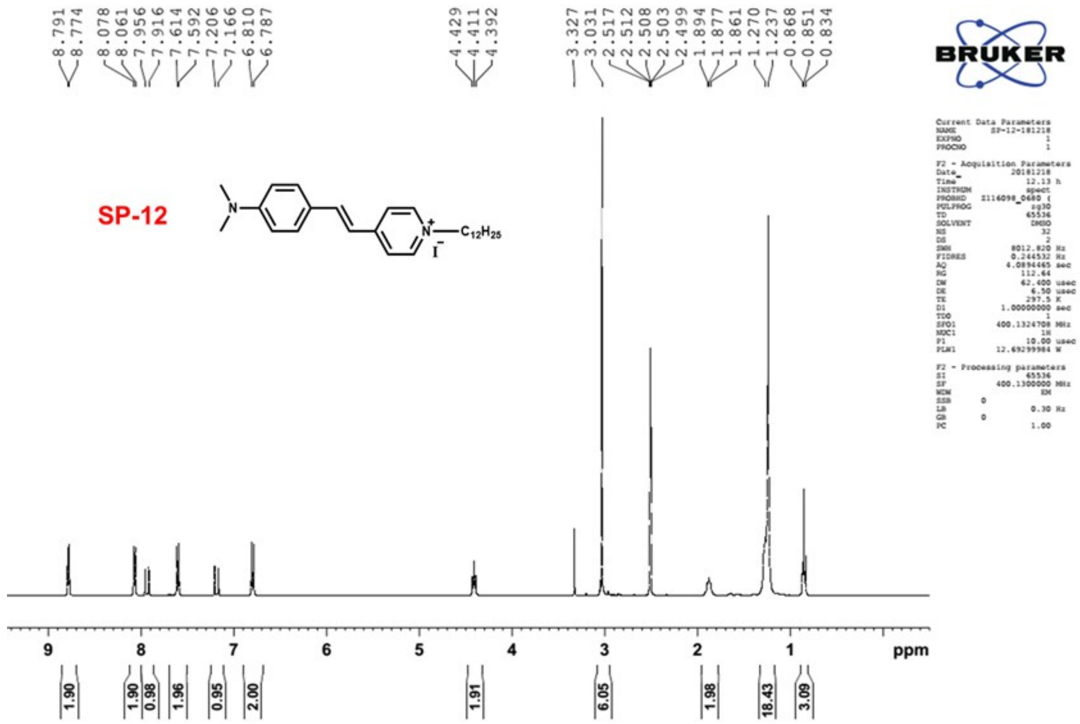

[1]H NMR spectrum of **SP-12** in DMSO-d_6.

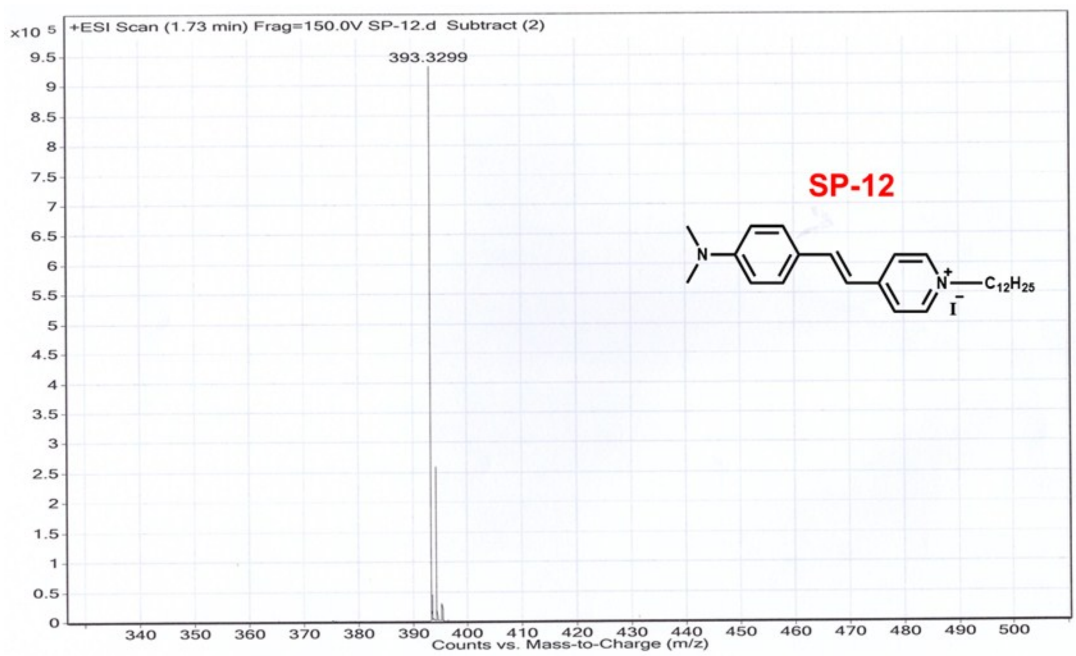

HRMS spectrum of **SP-12** in MeOH.

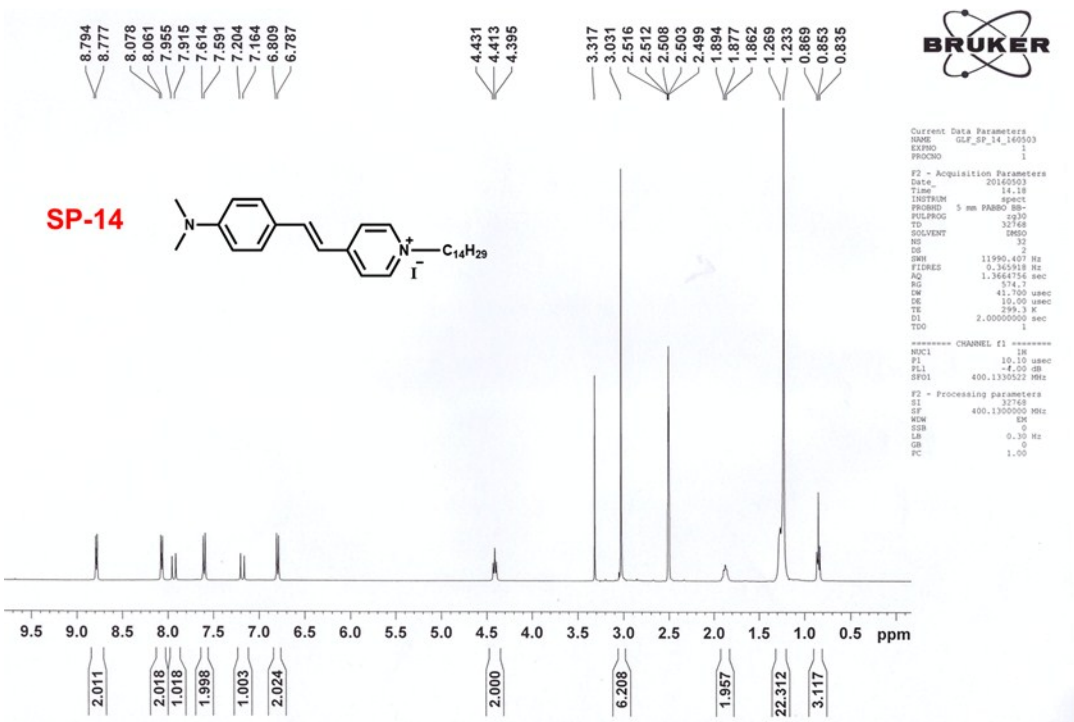

[1]H NMR spectrum of **SP-14** in DMSO-d_6.

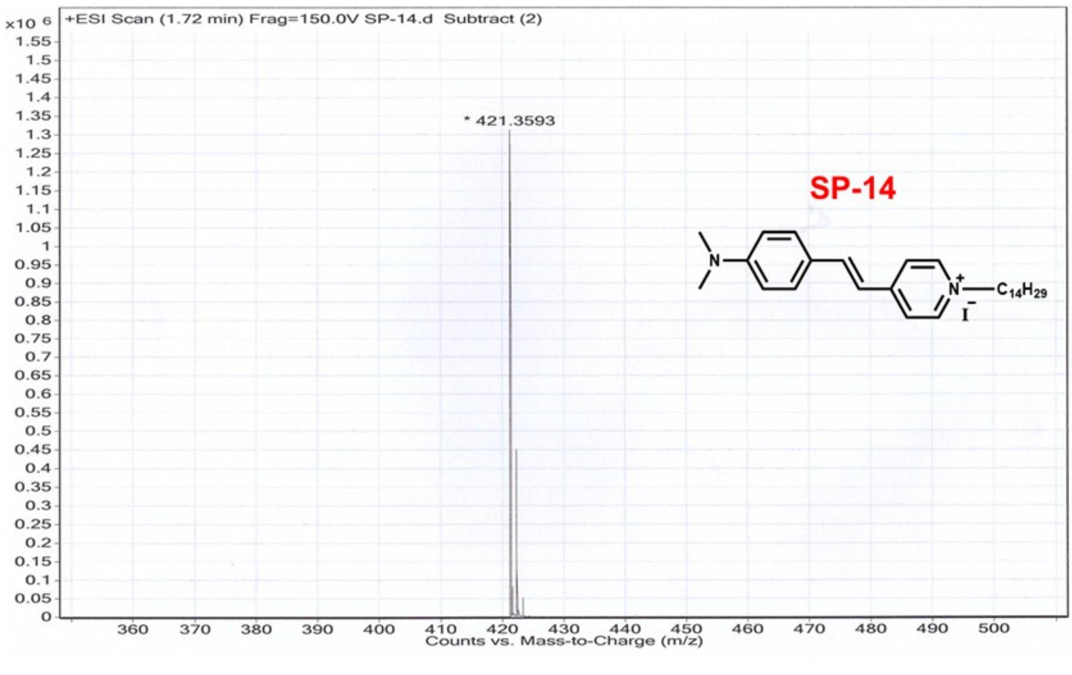

HRMS spectrum of **SP-14** in MeOH.

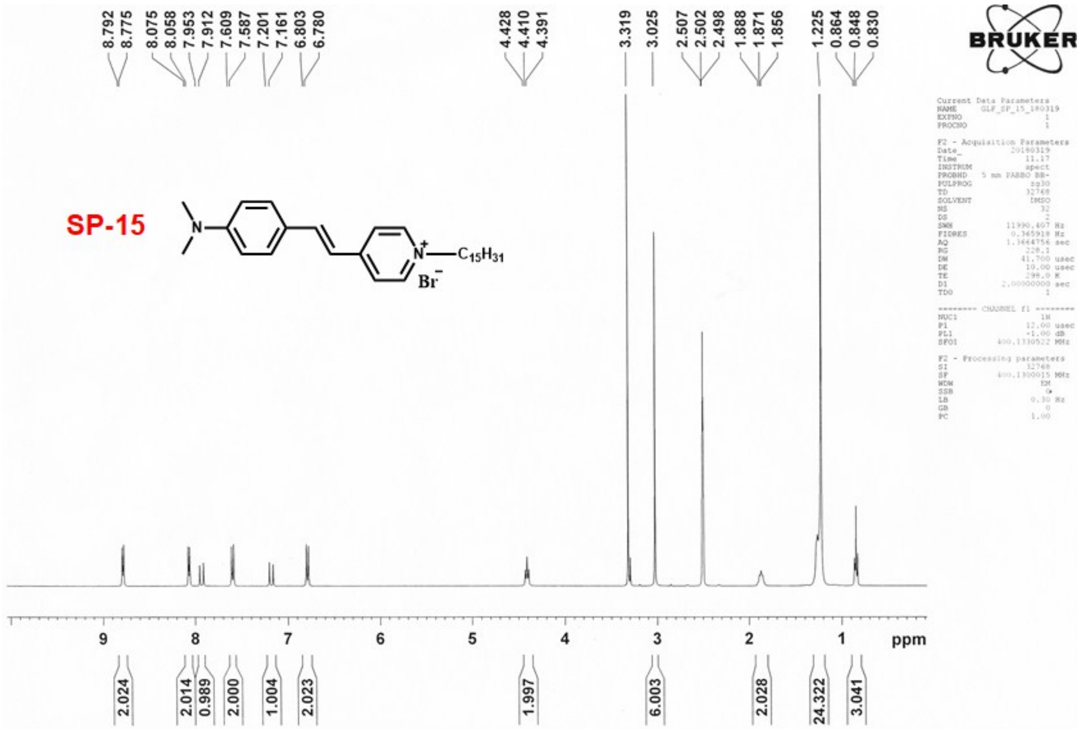

^{1}H NMR spectrum of **SP-15** in DMSO-d_6.

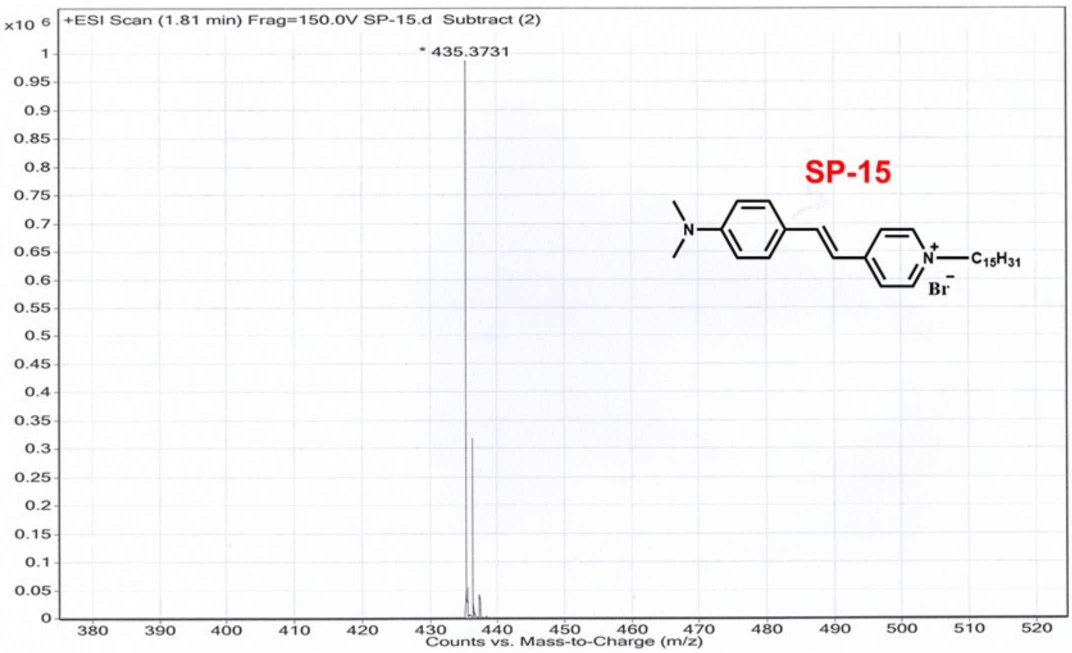

HRMS spectrum of **SP-15** in MeOH.

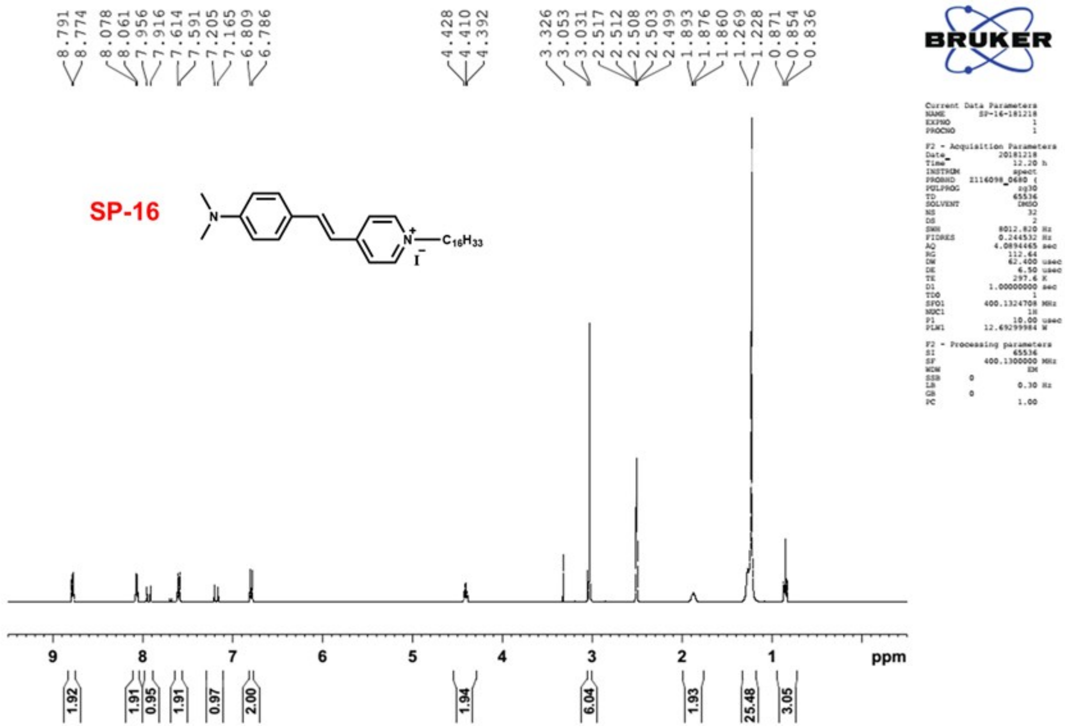

[1]H NMR spectrum of **SP-16** in DMSO-d_6.

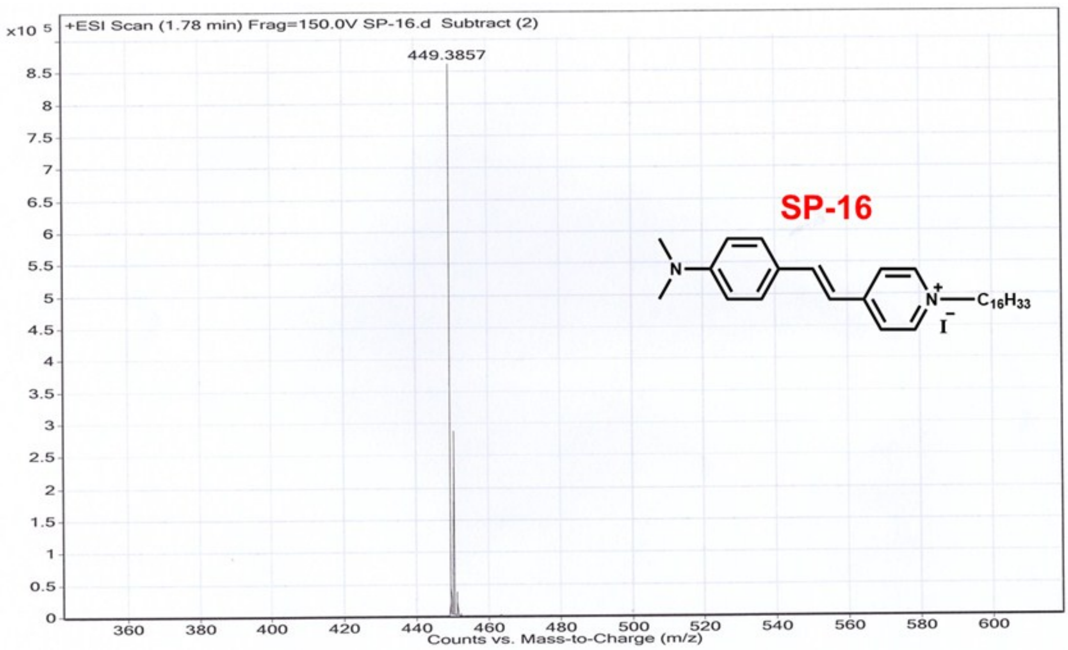

HRMS spectrum of **SP-16** in MeOH.

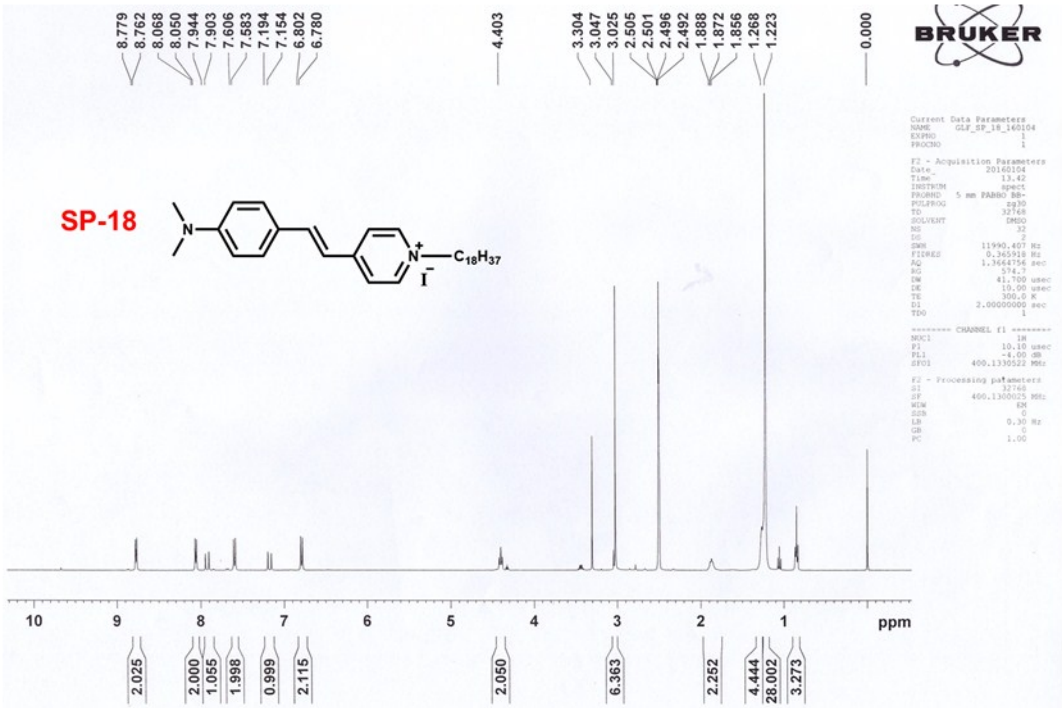

[1]H NMR spectrum of **SP-18** in DMSO-d_6.

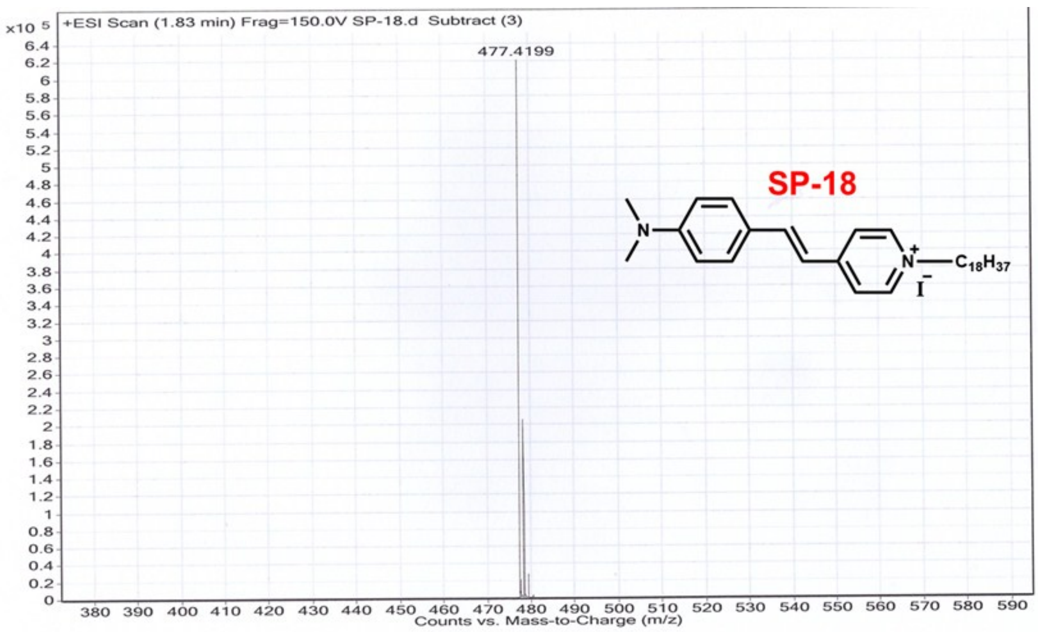

HRMS spectrum of **SP-18** in MeOH.

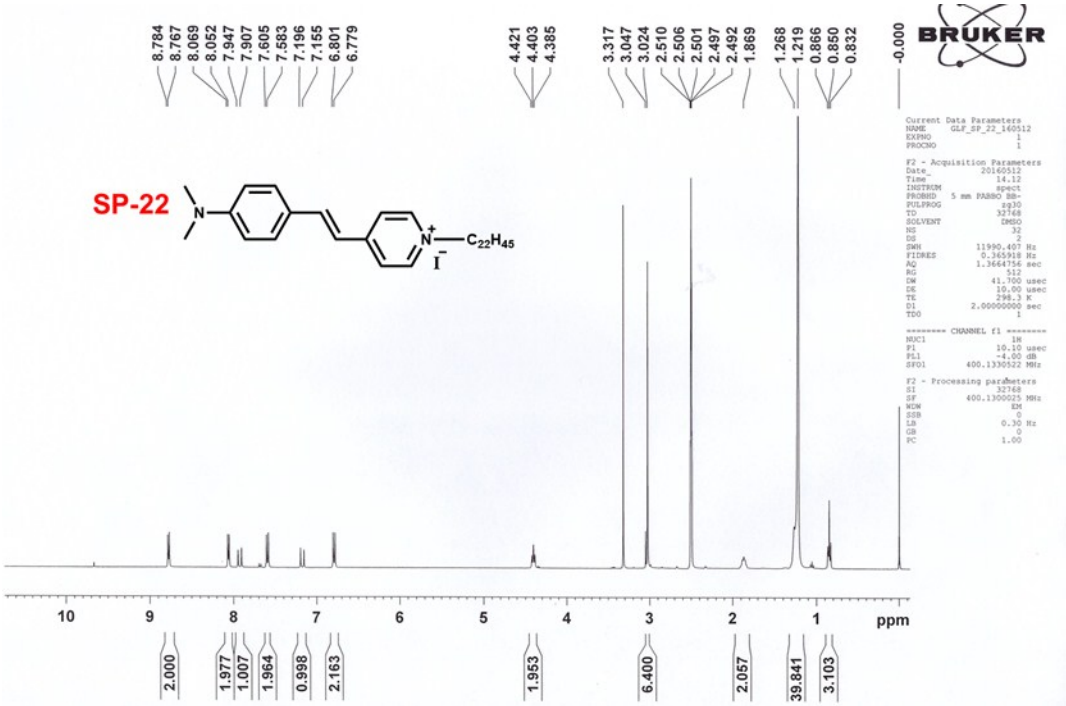

[1]H NMR spectrum of **SP-22** in DMSO-d_6.

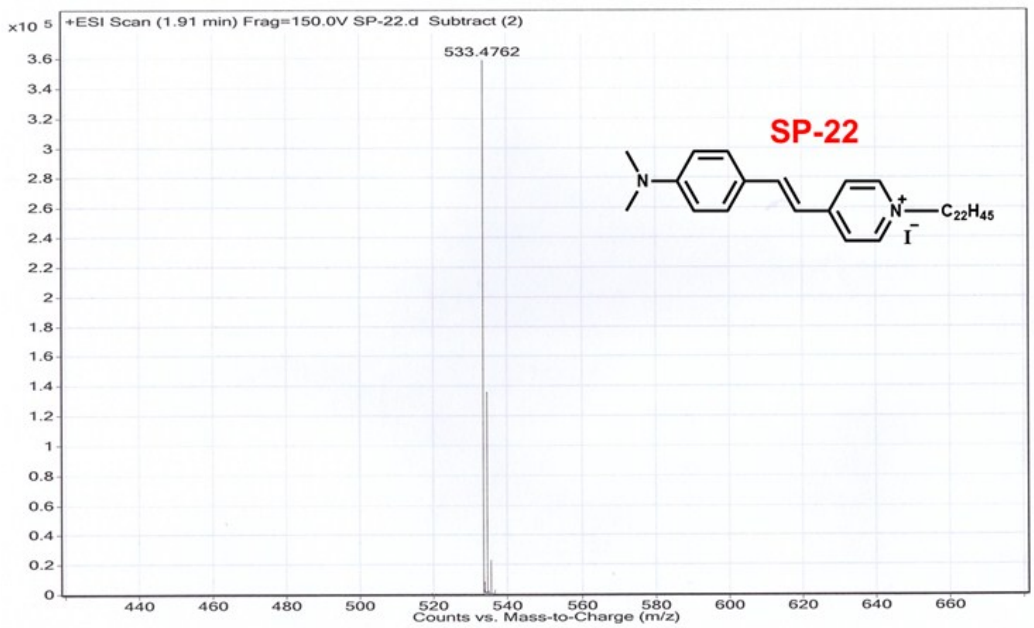

HRMS spectrum of **SP-22** in MeOH.

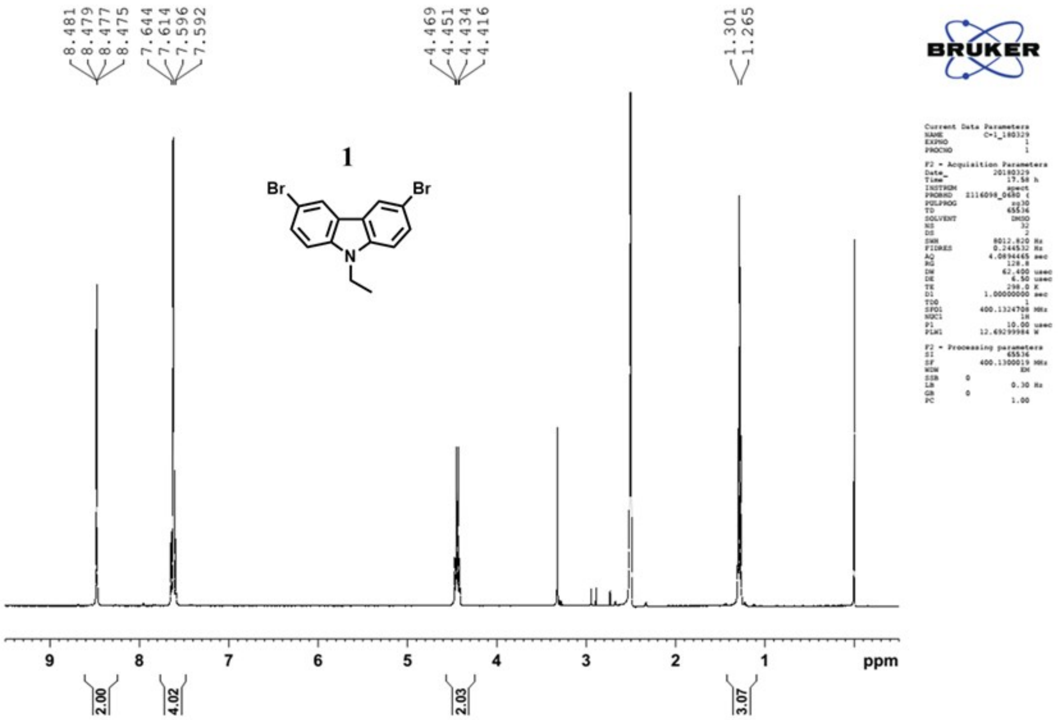

[1]H NMR spectrum of **1** in DMSO-d_6.

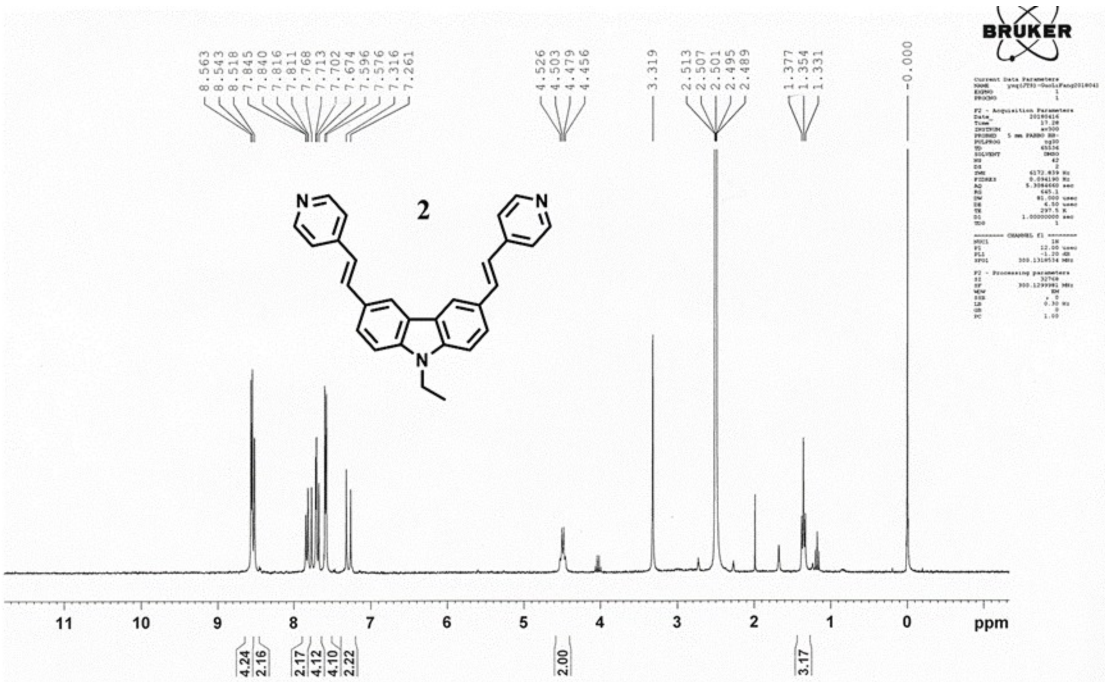

[1]H NMR spectrum of **2** in DMSO-d_6.

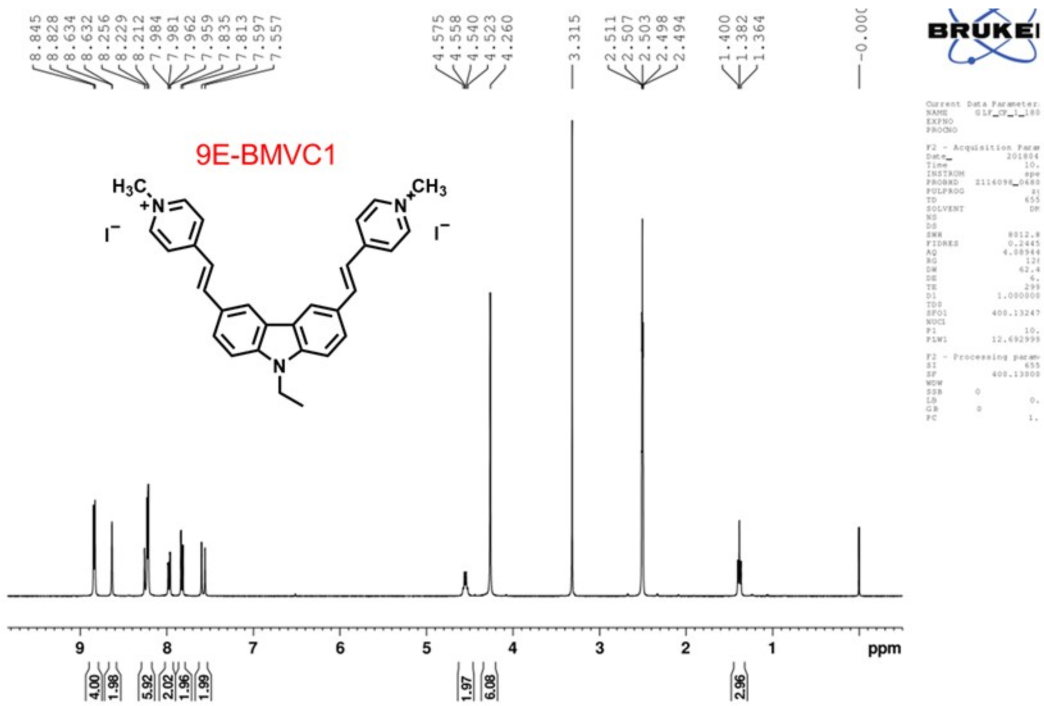

^{1}H NMR spectrum of **9E-BMVC1** in DMSO-d_6.

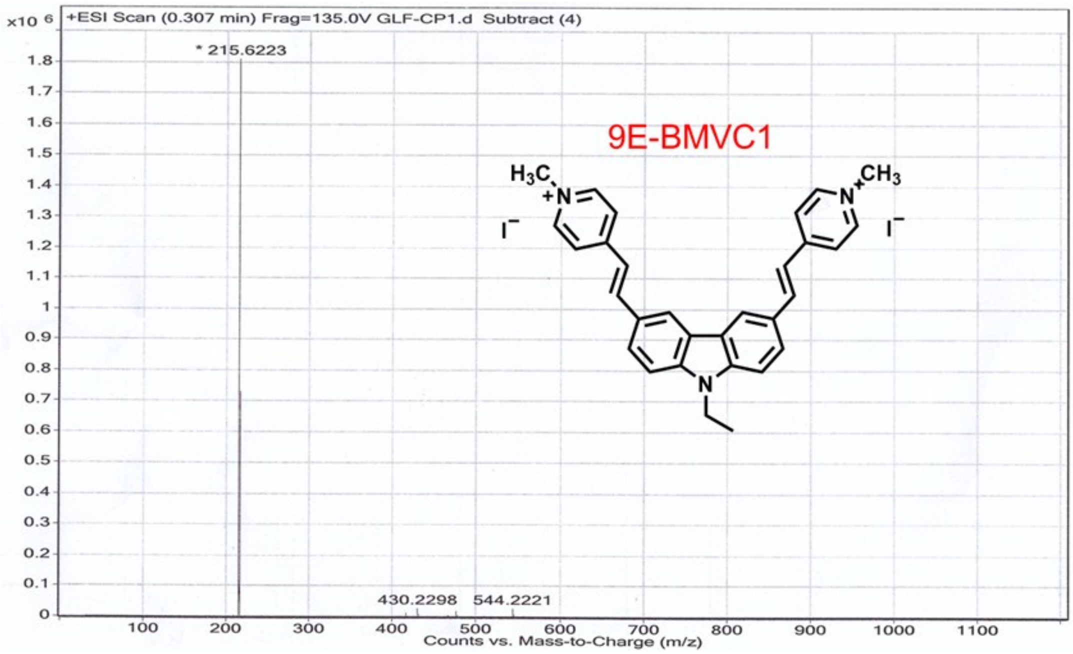

HRMS spectrum of **9E-BMVC1** in MeOH.

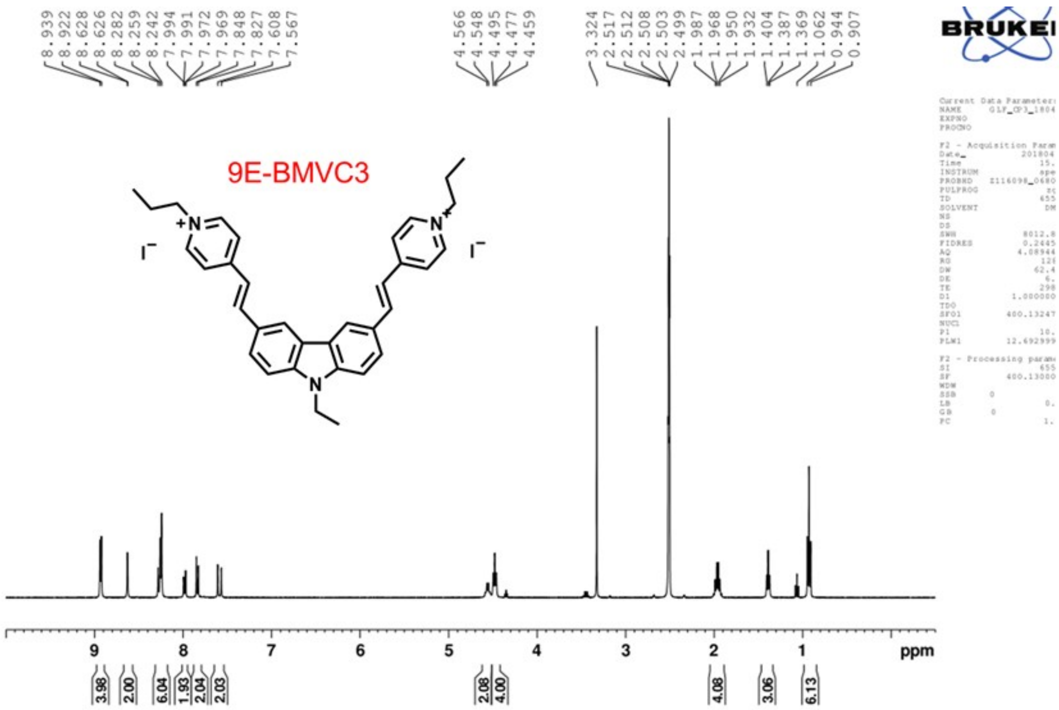

^{1}H NMR spectrum of **9E-BMVC3** in DMSO-d_6.

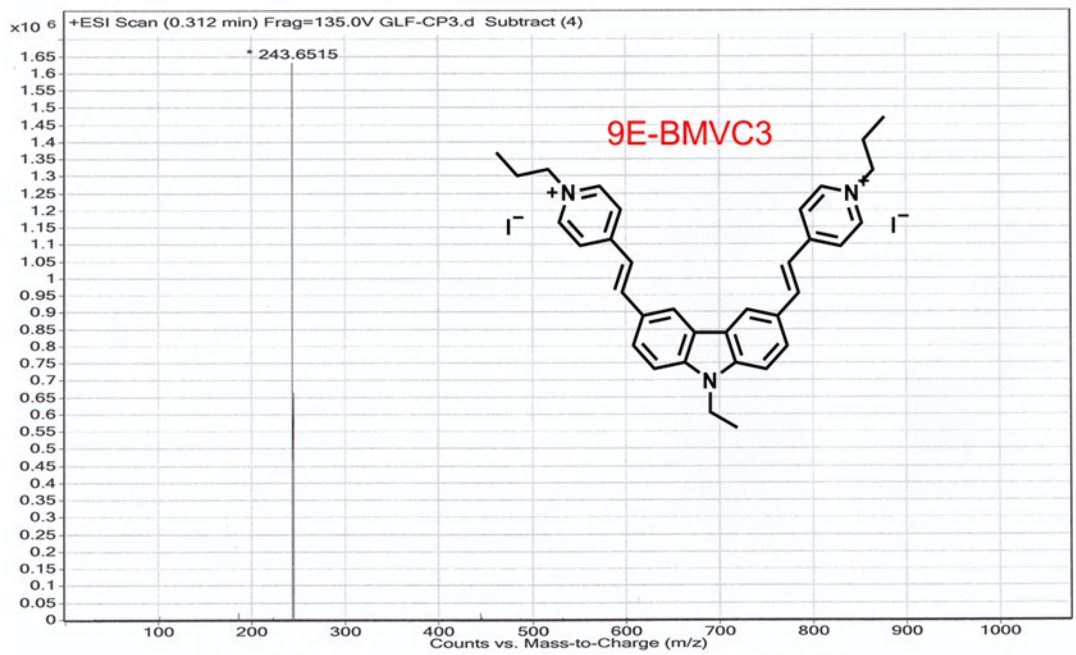

HRMS spectrum of **9E-BMVC3** in MeOH.

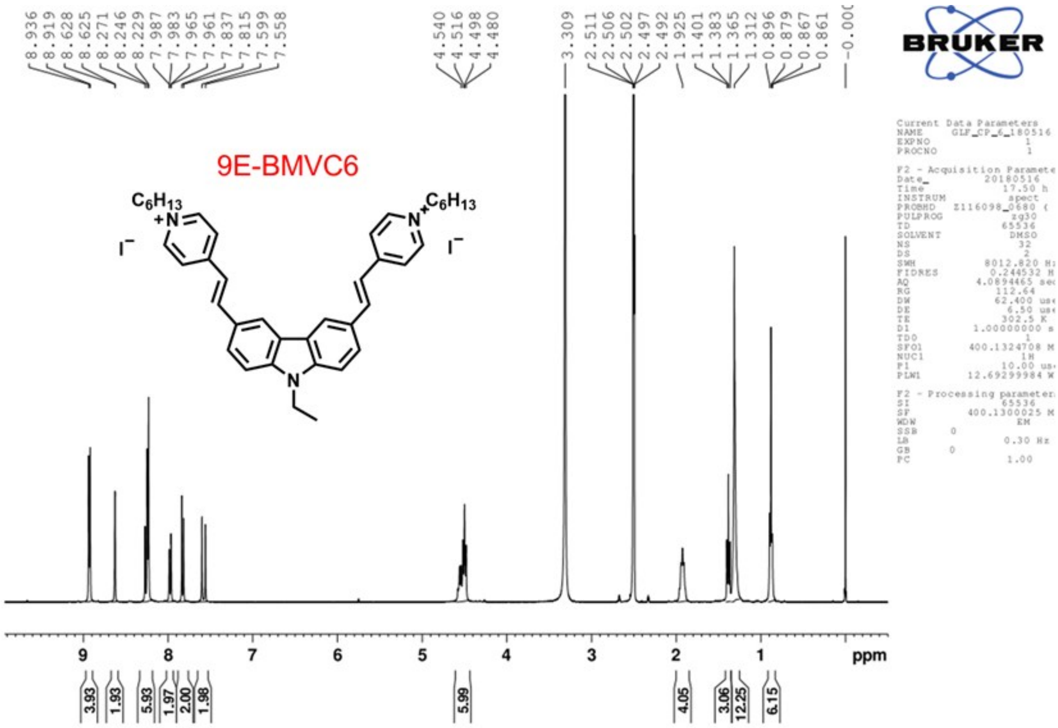

[1]H NMR spectrum of **9E-BMVC6** in DMSO-d_6.

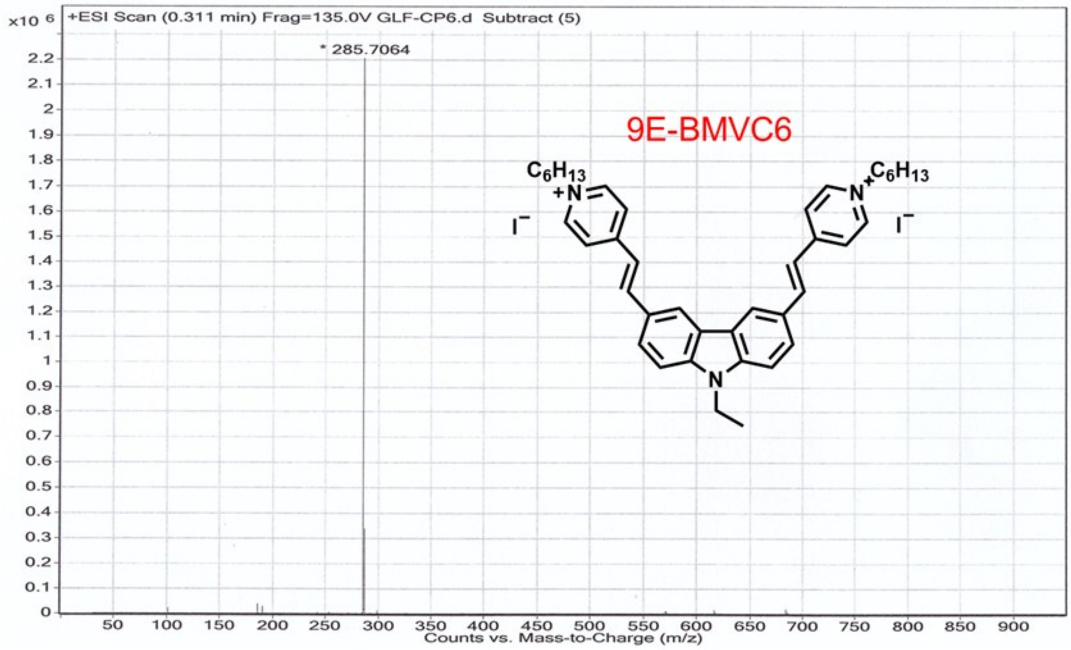

HRMS spectrum of **9E-BMVC6** in MeOH.

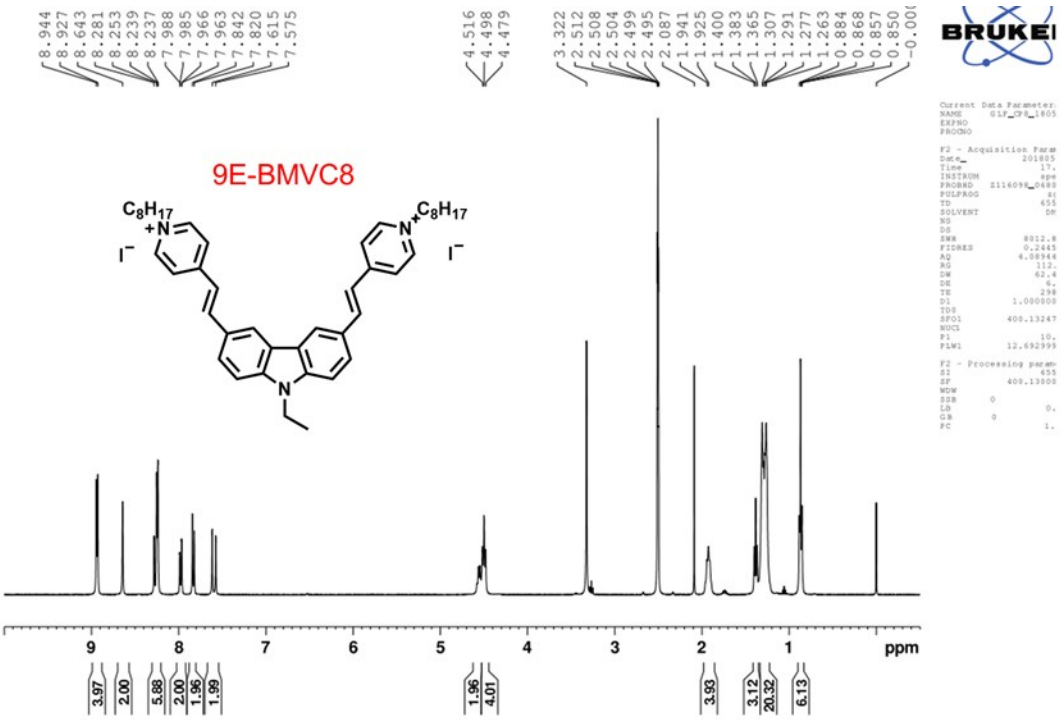

[1]H NMR spectrum of **9E-BMVC8** in DMSO-d_6.

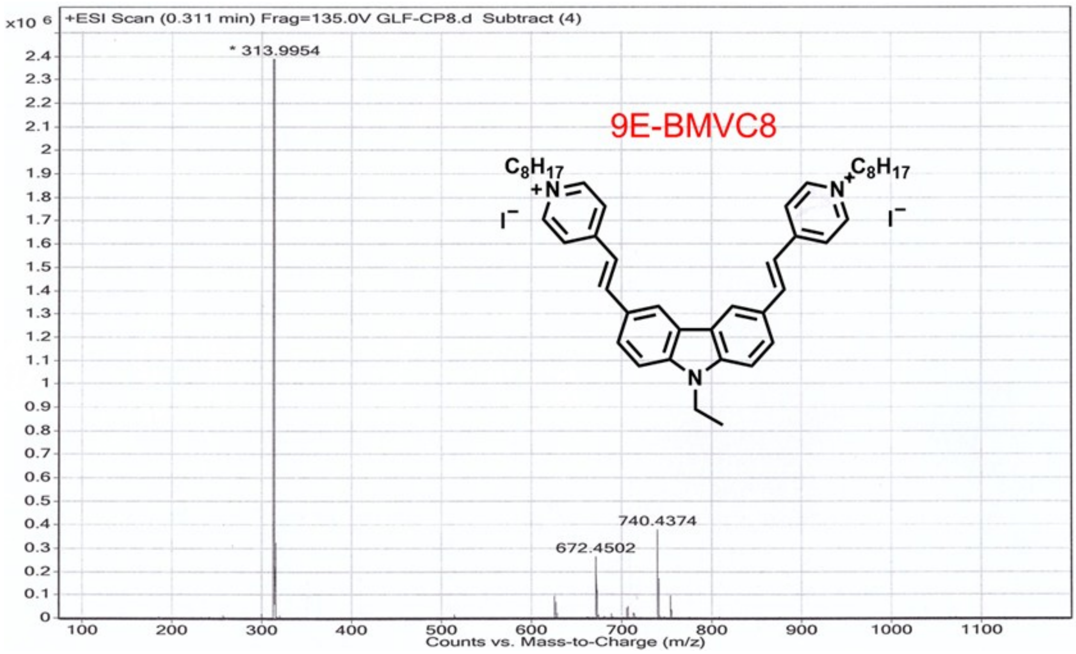

HRMS spectrum of **9E-BMVC8** in MeOH.

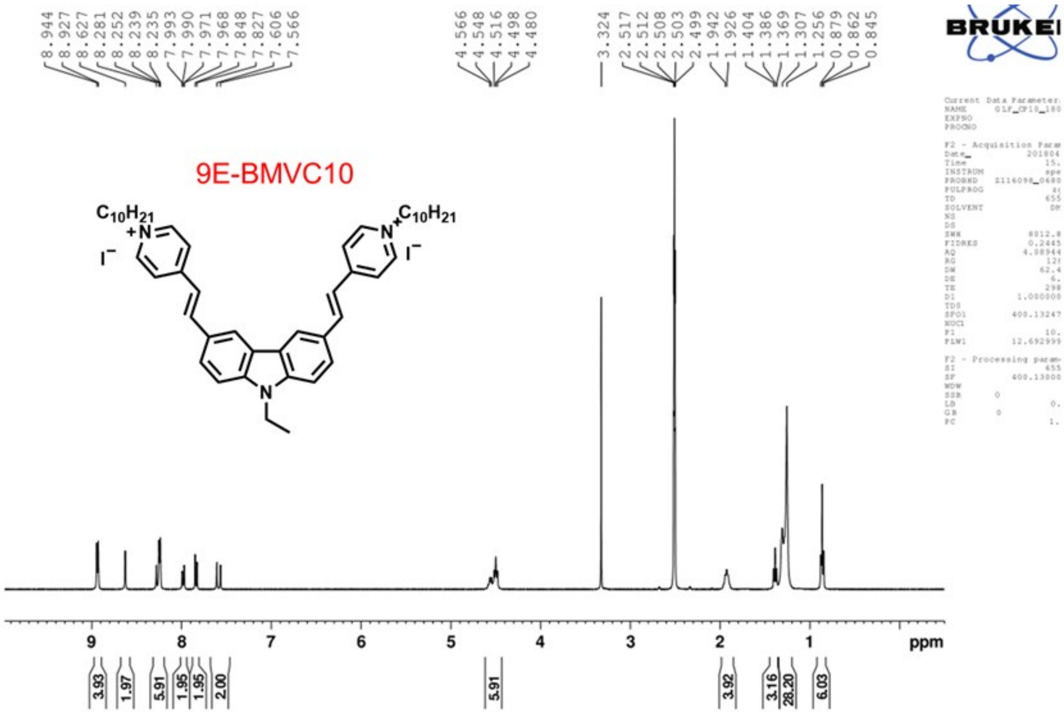

[1]H NMR spectrum of **9E-BMVC10** in DMSO-d_6.

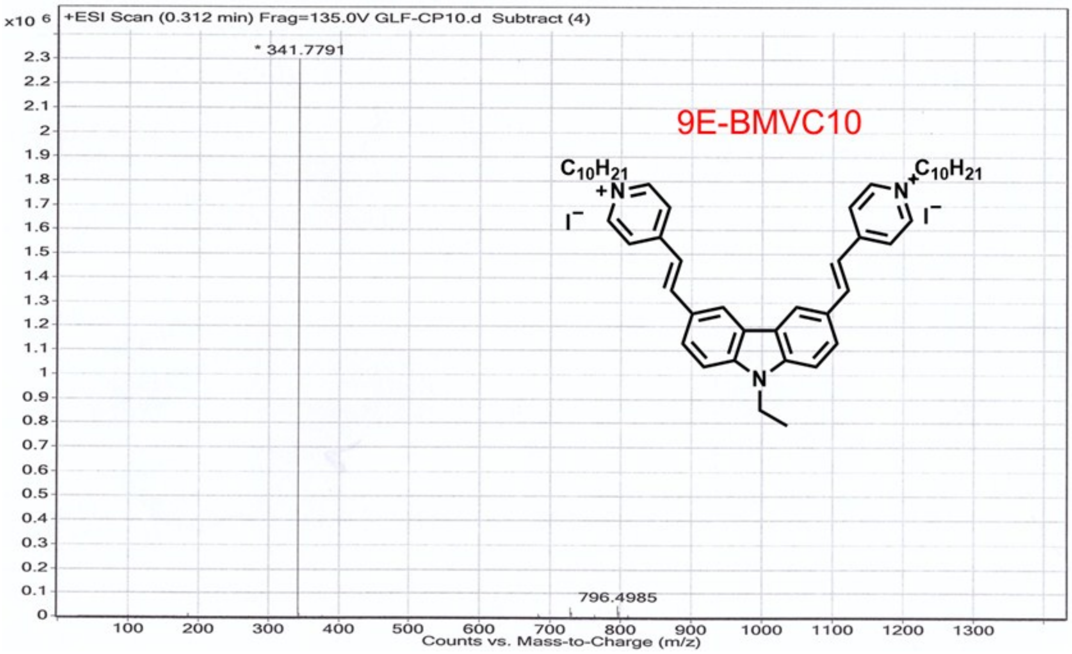

HRMS spectrum of **9E-BMVC10** in MeOH.

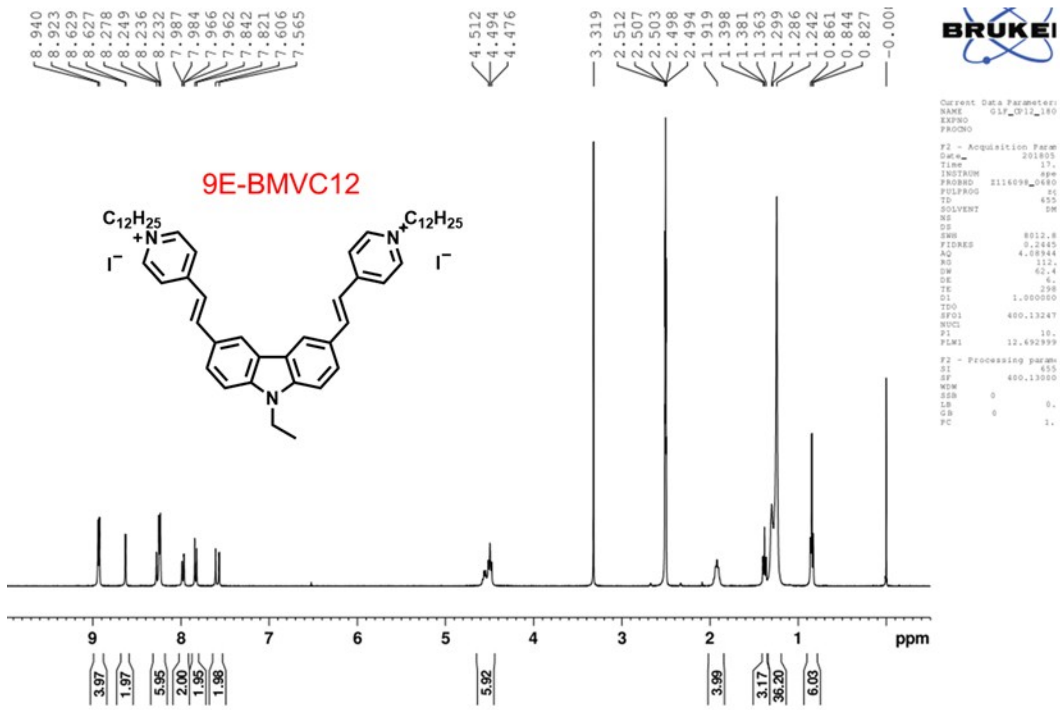

^{1}H NMR spectrum of **9E-BMVC12** in DMSO-d_6.

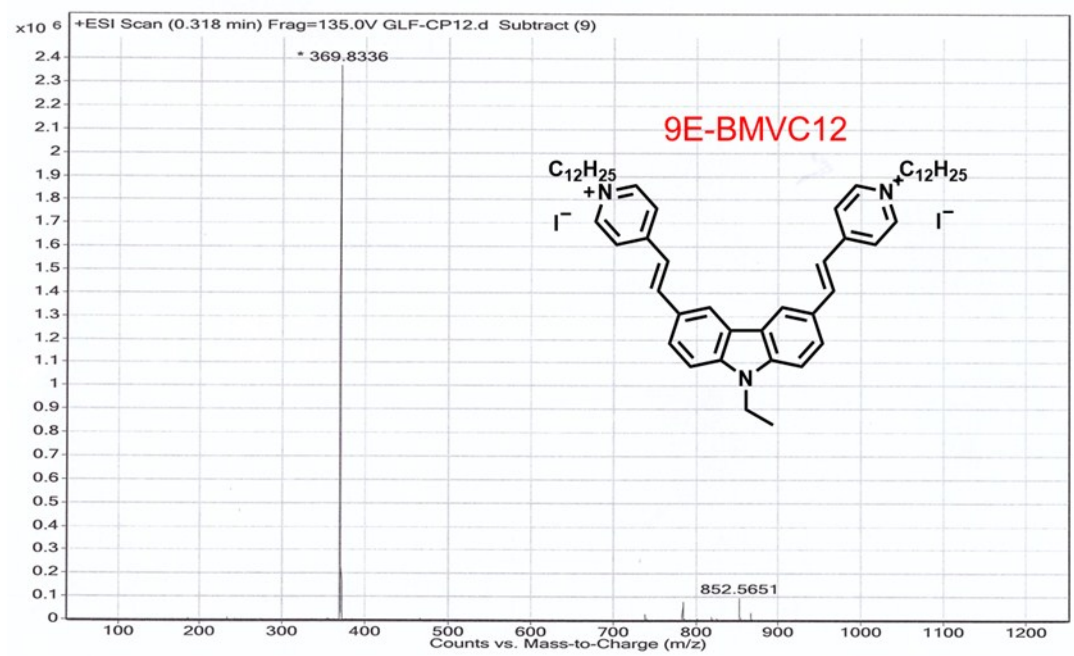

HRMS spectrum of **9E-BMVC12** in MeOH.